ISSN 1075-7015, Geology of Ore Deposits, 2019, Vol. 61, No. 5, pp. 391–421. © Pleiades Publishing, Ltd., 2019.
Russian Text © The Author(s), 2019, published in Geologiya Rudnykh Mestorozhdenii, 2019, Vol. 61, No. 5, pp. 3–36.

# Selenga Ore District in Western Transbaikalia: Structural–Minerogenic Zoning, Genetic Types of Ore Deposits, and Geodynamic Settings of Ore Localization

**I. V. Gordienko[a], *, R. A. Badmatsyrenova[a], V. S. Lantseva[a], and A. L. Elbaev[a]**

[a]*Geological Institute, Siberian Branch, Russian Academy of Sciences, Ulan-Ude, 670047 Russia*

**e-mail: gord@pres.bscnet.ru*

Received April 19, 2018; revised May 28, 2018; accepted February 27, 2019

**Abstract**—Integrated structural geological, minerogenic, and metallogenic studies with allowance for previous topical surveying, geological mapping and prospecting, and mineral exploration data has revealed that Upper Paleozoic and Early Mesozoic tectonomagmatic structures are widespread in the Selenga ore district. They are associated with the evolution of the transregional Upper Paleozoic Selenga–Vitim rift-related volcanoplutonic belt and the formation of the Early Mesozoic West Transbaikalian region of intraplate magmatism. Late Paleozoic–Mesozoic igneous activity accounts for the bulk of mineable mineral resources in the Selenga ore district concentrated inside and outside the ore clusters (Kunalei, Kizhinga, Cheremshana–Oshurkovo, Tashir, etc.). It is demonstrated that the main mineable metals in the district are molybdenum and beryllium, which determine the minerogenic specificity of the ore district. New compositional characteristics of the Upper Paleozoic and Early Mesozoic intraplate magmatic complexes and the associated mineral deposits (Mo, Be, Ti, quartz, fluorite, and apatite ores), as well as other promising gold, uranium, and REE–Ba–Sr ore occurrences were obtained. The geodynamic settings of their formation and the ages of the main ore-forming processes have been established; the viability of the mining industry in the Selenga ore district and the feasibility of involving its ore potential in the district's economic modernization program have been assessed.

*Keywords:* geological structure, ore district, strategic minerals, structural–minerogenic zoning, genetic types of ore deposits, outlook for economic development

**DOI:** 10.1134/S1075701519050027

## INTRODUCTION

The Selenga ore district is located in the central part of the Republic of Buryatia. It occupies the southern and southwestern parts of Western Transbaikalia and covers 48000 km$^2$. The structural pattern of the district is defined by its location in the Sayan–Baikal Fold Belt, which encircles the Siberian Craton in the south. Geological studies of this vast and easily accessible territory east of Lake Baikal has a long history, starting from the first adventurers and academic expeditions of Tsarist Russia to the most active work during the postwar development of the USSR and modern Russia. In the 1960s and later, geological, tectonic, and minerogenic surveys were carried out in Western Transbaikalia, including the Selenga ore district. Their results are discussed in monographs by A.D. Shcheglov (1966); P.M. Khrenov et al. (1966), V.V. Skripkina et al. (1982); E.E. Baturina and G.S. Ripp (1984); K.B. Bulnaev (1995); I.V. Gordienko (1970, 1976, 1987, 1992, and 2014); V.V. Yarmolyuk et al. (1998 and 2001); V.I. Kovalenko et al. (2003); V.I. Ignatovich (2007); G.S. Ripp et al. (2000 and 2013); V.I. Bakhtin et al. (2007); V.S. Platov et al. (2009); D.A. Lykhin and V.V. Yarmolyuk (2015); etc. A number of ore clusters with different mineralization types and potential resources have been recognized in the Selenga ore district based on the results of these studies and industrial geological mapping/prospecting and mineral exploration surveys.

The preliminary data of our investigations were summarized in a brief review without any cartographic materials illustrating the geological structure of individual mineral deposits and ore occurrences in the ore district (Gordienko et al., 2018a).

This paper, in addition to the overview of the geological structure and the structural–minerogenic zoning of the Selenga ore district, presents details of the structure, composition, and potential resources of more than 20 individual ore deposits and large occurrences of metallic and nonmetallic strategic minerals of various genetic types (Mo, Be, Ti, quartz, fluorite, and apatite ores), as well as other promising copper, gold, uranium, and REE–barium–strontium ore occurrences. The geodynamic settings of their forma-

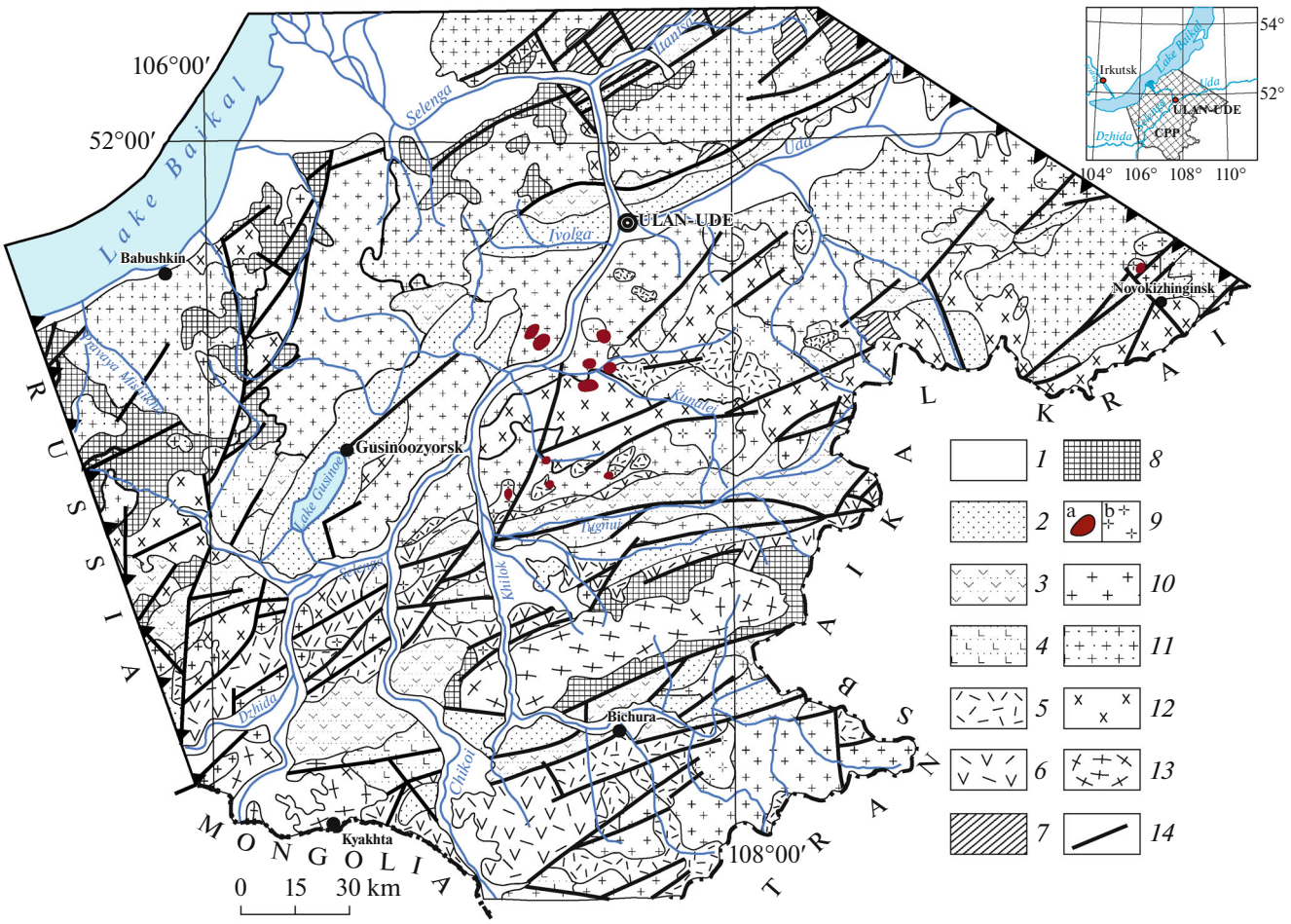


**Fig. 1.** Geological sketch map of Selenga ore district. Compiled using Geological Map of Southern East Siberia and Northern Mongolian People's Republic (1980); State Geological Map of Russian Federation (Platov et al., 2009); reports on geological mapping surveys of PGO Buryatgeologiya, with authors' additions. *Stratified sedimentary and volcanic rocks*: (*1*) Neogene–Quaternary clastics and volcanics, Ng-Q; (*2*) Early Cretaceous sedimentary and volcanic rocks and carbonatites in rift troughs (Gusinoozyorsk Group, Khilok Formation, Khalyuta Complex), $K_1$; (*3*) Jurassic sedimentary and volcanic rocks in rift troughs (Tugnui, Ichetuy, and Baikal formations), J; (*4*) Middle–Late Triassic sedimentary and volcanic rocks (Chernoyarovo and Tsagan–Khuntei formations), $T_{2-3}$; (*5*) Late Permian volcanics (Alentui and Tamir formations), $P_2$; (*6*) Late Carboniferous–Early Permian volcanic and volcanosedimentary rocks (Gunzan and Ungurkui formations), $C_3$–$P_1$; (*7*) Devonian–Carboniferous clastic–carbonate sediments (Tataurovo and Udunga formations), D–C; (*8*) Neoproterozoic–Cambrian metaclastic rocks (Temnik and Astai formations), NP–Є; (*9–13*) *Intrusive complexes:* (*9*) Middle–Upper Triassic Sogota and Late Kunalei complexes of leucocratic granites, porphyry granites and syenites, and explosive breccias, $\gamma$-$\gamma\pi$-$\varepsilon\pi T_{2-3}$ (a) and Late Permian–Early Triassic Kunalei Complex of subalkaline and alkaline granites and syenites, $\gamma$-$\varepsilon P_2$-$T_1$ (b); (*10*) Early–Late Permian Bichura and Zaza complexes of granites, leucogranites, and quartz syenites with basites, $\gamma$-$\varepsilon\gamma P_{1-2}$; (*11*) Middle–Late Carboniferous Barguzin Complex of auto- and allochthonous granites, $\gamma C_{2-3}$; (*12*) Early Paleozoic Dzhida Complex of accretionary–collisional granitoids, $\gamma\nu PZ_1$; (*13*) Proterozoic Zagan granite–metamorphic complex, $\mu PR$; (*14*) normal, strike-slip, and thrust faults. Inset map shows location of Selenga ore district (SOD).

tion and the ages of the main ore-forming processes have been established; the viability of the mining industry in the Selenga ore district and the feasibility of including its ore potential in the district's economic modernization program have been assessed.

Our investigations focused on the geological structure, minerogenic zoning, ore cluster characteristics, genetic types of ore deposits, geodynamic settings of their formation, and the outlook for further economic development of the Selenga ore district in the Republic of Buryatia.

## GEOLOGICAL STRUCTURE

The structure of this territory is characterized by the presence of the Baikalide, Caledonide, Hercynide, and Mesozoide (Cimmeride) structural–stratigraphic complexes. The present boundaries of these complexes are controlled by large northeast–southwest and submeridionally trending faults with mostly strike-slip movement (Fig. 1).

The Baikalide (Neoproterozoic) blocks are exposed mostly within the Khamar–Daban and Mor-

skoi ranges along coast of Lake Baikal and in the Kyakhta and Zagan metamorphic basement highs in the south. They are composed of metasedimentary rocks of the Khangarul, Selenga, and Kyakhta groups crosscut by occasional syncollisional granitoid bodies (Zagan Complex), whose age has not yet been determined with confidence and is considered as ranging from the Early Proterozoic to the Devonian inclusive (Platov et al., 2009).

The Caledonide (Vendian–Early Paleozoic) complexes within the Selenga ore district are fragments of marginal sedimentary basins (the Temnik, Astai, and Kunalei formations) of the Uda–Vitim and Dzhida island-arc systems, which display a transform junction with each other along a series of submeridionally trending strike-slip faults identified west of the Gusinoozyorsk Depression. The geology and metallogeny of these island-arc systems was discussed earlier (Platov et al., 2009; Gordienko et al., 2010; Gordienko and Nefed'ev, 2015; Gordienko et al., 2018b).

The Upper Paleozoic (Hercynide) and Mesozoic (Cimmeride) tectonomagmatic structures are the most widespread within the Selenga ore district. They are related to the development of the transregional Upper Paleozoic ($C_2$–$P_1$) Selenga–Vitim (Mongolia–Transbaikalia) rift-related volcanoplutonic belt and the formation of the Mesozoic ($T_{2-3}$–$K_1$) West Transbaikalian domain of rift-related (intraplate) magmatism (Gordienko, 1976, 1987; Gordienko and Kuzmin, 1999; Yarmolyuk et al., 2001, 2002, and 2017).

The first outbursts of Upper Paleozoic magmatism in the study area were related to the inception of the Selenga–Vitim volcanoplutonic belt. They are represented by large-scale trachyandesite–basalt–rhyolite volcanism and volcaniclastic sediment accumulation in rift troughs (the Gunzan, Ungurkui, and Surkhebta formations, $C_2$–$P_1$) and the emplacement of calc-alkaline crustal granitoid intrusions of the Barguzin Complex (330–290 Ma) followed, after a short interruption, by the subalkaline and normal alkaline granitoids of the Zaza and Bichura complexes with ages between 305 and 285 Ma. The mass emplacement of granitoids of the Angara–Vitim areal pluton (batholith) occurred during this stage. Furthermore, the granitoids of the Barguzin Complex of the early phase (325–290 Ma) of the Angara–Vitim batholith emerged within a vast area (~ 150000 km$^2$) in Western Transbaikalia and "sutured" the Early Caledonide complexes of the Uda–Vitim island-arc system. The influence of the batholith-related granitoids, the Zaza complex in particular, extended from the upper reaches of the Vitim River to the Selenga River basin and further into the Dzhida ore district (Gordienko et al., 2018b; Tsygankov et al., 2017).

This was followed, almost without interruption and especially in the Selenga ore district, by the resumption of igneous activity that led to the formation of vast Upper Permian volcanic fields (Alentui and Tamir formations) and volcanotectonic structures saturated with comagmatic subalkaline and alkaline granitoids during the Late Permian and Early and Late Triassic times (Kunalei, Late Kunalei, and Sogota complexes). The vast Selenga–Vitim (Mongolia–Transbaikalian) magmatic domain, immediately adjacent to the Selenga ore district, was formed during this time. The core of the domain is the Khentei–Dauria batholith dated at 230 to 195 Ma (Kovalenko et al., 2003). The formation of the Khentei–Dauria zoned domain in Southwestern Transbaikalia was accompanied by active volcanic processes that led to the deposition of the Chernoyarovo, Tsagan–Khuntei, and Ichetuy volcanic sequences of predominantly bimodal trachybasalt–trachyrhyolite rock series and the comagmatic alkali granitoids (Gordienko et al., 2018b; Gordienko and Kuzmin, 1999; Yarmolyuk et al., 2002).

Starting from the Late Triassic, Jurassic, and Early Cretaceous, the entire territory of the ore district was involved in the development of the West Transbaikalian domain of rift-related (intraplate) magmatism. These processes led to the inception of numerous troughs and horstlike uplifts with powerful trachybasalt eruptions, the formation of stratovolcanoes, and accumulation of bimodal trachybasalt–trachyrhyolite–comendite volcanic series in association with diverse basites and granitoids. Many authors who studied the Late Carboniferous–Permian–Triassic alkali granite magmatism in Western Transbaikalia note the unusual duration (~120 My) of these igneous processes within a relatively small region (Litvinovskii et al., 2001; Yarmolyuk et al., 2001; Tsygankov et al., 2010; Jahn et al., 2009; Reichow et al., 2010).

Large volcanoplutonic structures with an area of up to 2000 km$^2$ formed in the Selenga ore district during this period, consisting of fields of alkaline–bimodal volcanics (Tsagan–Khuntei and Chernoyarovo formations) and massifs of alkali granites and syenites of the Late Kunalei and Sogota complexes dated at 230–210 Ma (Khambin and Tsagan–Daban ranges, Tugnui Depression, etc.) (Gordienko and Klimuk, 1995; Vorontsov and Yarmolyuk, 2007; Andryushchenko et al., 2010). Widespread Middle–Late Triassic plutonic and volcanic rocks in an extensive belt; the large thicknesses of volcanic sequences of trachybasalts, trachytes, trachyrhyolites, and comendites; and the presence of rift grabens and extensive basalt–comendite dike belts associated with alkaline granitoids are evidence of the relationship between this intraplate magmatism and plume sources (Gordienko et al., 2018b; Yarmolyuk et al., 2017; Tsygankov et al., 2010; Yarmolyuk et al., 2000; Kuzmin and Yarmolyuk, 2014).

The emplacement of Late Jurassic subalkaline granite-gneisses (Mangirtui and other massifs) and the inception of the Tugnui and Chikoi–Khilok rifts during the Late Mesozoic were associated with exhumation of Proterozoic thickened crust and formation

of Cordillera-type granite–metamorphic nuclei within the Zagan Range and the Kyakhta high (Donskaya et al., 2008). At the same time, alkaline and subalkaline volcanic and subvolcanic igneous rocks and associated carbonatite ledges dated at 115–130 Ma formed at the same time in fault-related pull-apart structures along the margins of Late Jurassic–Early Cretaceous depressions in Western Transbaikalia (Nikiforov et al., 2000, 2002; Ripp et al., 2000).

It is assumed that the bulk of economic (mineable) resources of the strategically important mineral deposits of the Selenga ore district are associated with Late Paleozoic–Early Mesozoic magmatism.

## STRUCTURAL–MINEROGENIC ZONING

The Selenga ore district was recognized after detailed geological mapping and metallogenic surveys in southern Western Transbaikalia (Baturina and Ripp, 1984). Later it was classified as part of the large Selenga–Vitim structural–minerogenic zone (Ignatovich, 2007), which is associated with the development of the transregional Upper Paleozoic Mongolian–Transbaikalian rift-related volcanoplutonic belt (Gordienko, 1987, 1992). The Selenga–Vitim zone occupies the central position in the ore district and borders the Cisbaikal and Chikoi–Ingoda structural–minerogenic zones of the Selenga ore district in the northwest and southeast, respectively. The priority mineralization for the Selenga–Vitim zone is molybdenum and beryllium ores and fluorite in the Kunalei, Kizhinga, Novopavlovka, and Tashir ore clusters. Similar ore formation processes took place in the Tamir ore cluster in the Chikoi–Ingoda zone. The Cisbaikal zone contains mostly nonmetallic minerals (quartzites, aptite) and carbonatites (Fig. 2).

Starting from 1960s–1980s, mineral prospecting and exploration of the discovered ore deposits and occurrences in the Selenga ore district was carried out for a long time by numerous crews of mapping geologists and mineral exploration specialists of the Buryatian Geological Administration (D.D. Sagaluev, V.A. Novikov, O.V. Sokolov, A.A. Karbainov, A.K. Izvekov, V.E. Leonov, L.I. Leshukov, V.S. Platov, V.V. Koshkin, V.V. Skripkina, E.E. Baturina, V.L. Vernik, V.F. Barskii, Yu.P. Gusev, and others) along with scientific research institutes and, in recent years, commercial organizations. As a result, a number of ore clusters with different mineralization types and potential resources were recognized within the Selenga ore district. Twenty-four mineral deposits, almost 70 occurrences and more than 70 mineralized points were discovered therein. As obvious from the sketch map in Fig. 2, the main mineable metals and minerals in the district are beryllium, molybdenum, titanium, quartz, fluorite, and apatite. Copper, gold, uranium, and rare earth–barium–strontium ores are less widespread. Mineral deposits are concentrated in large ore clusters (Kunalei, Kizhinga, and Cheremsnany–Oshurkovo), and promising underexplored ore occurrences, within or outside smaller ore clusters (Tashir, Novopavlovka, Tamir, etc.).

As a result of active intraplate (rift-related) processes in the Selenga ore district, a number of endogenic rare metal, titanium, gold, rare-earth elements, and nonmetallic mineral deposits of postmagmatic and hydrothermal–metasomatic genesis formed. The leading roles in these processes were played by mantle plumes and abyssal transmagmatic solution (fluid) flows, which concentrated in the upper horizons of ore-magmatic systems, in dike and fault zones. The action of plumes obviously continued for a long time, from the Late Paleozoic to the Mesozoic inclusive, and was impulsive. This accounts for the different ages of igneous events and ore-emplacement processes at virtually all ore deposits and occurrences of the Selenga ore district.

## GENETIC TYPES AND GEOLOGICAL STRUCTURE OF MINERAL DEPOSITS

It has been established that the molybdenum and beryllium ores determine the metallogenic pattern of the studied ore district. Therefore, let us discuss these mineral deposits and occurrences in more detail. Large strategic nonmetallic mineral deposits (Cheremshanskoe quartzite, Oshurkovskoe apatite, and numerous fluorite deposits) have been studied in sufficient detail and described in numerous publications available in the public domain. They are briefly mentioned in this paper and require special comprehensive analysis in the future. Their basic parameters are given in Table 1.

**Molybdenum.** Molybdenum deposits and occurrences are attributed to the plutonogenic–hydrothermal genetic type. The sources of molybdenum mineralization are Late Paleozoic–Early Mesozoic peralkaline volcanoplutonic associations of the Selenga ore district. The following ore formation types have been recognized: (1) porphyry molybdenum: Zharchikhinskoe, Kharitonovskoe, Kolobkovskoe, Leonovskoe, Nadeinskoe, Novopavlovskoye, and some others; (2) molybdenum–quartz–greisen: Ivanovskoe, Tamirskoe, Khambinskoe, Sheno-Baidal, Shaloty, Gudzhertuiskoe, and other smaller occurrences; (3) porphyry copper–molybdenum: Malo-Kudarinskoe and Kudarinskoe. Most molybden-bearing deposits are attributed to the porphyry molybdenum type and are concentrated in the Kunalei ore cluster.

*The Zharchikhinskoye molybdenum deposit* was discovered in 1978 as a result of 1 : 50000 geological mapping surveys (Karbainov et al., 1979unp[1]). In 1979–1983, this area was successively covered by geological

[1] Hereafter "unp" designates unpublished reports (manuscripts) kept in the Buryatian Branch of the Federal State-Funded Institution "Territorial Archive of Geological Information (TAGI) for the Siberian Federal District."

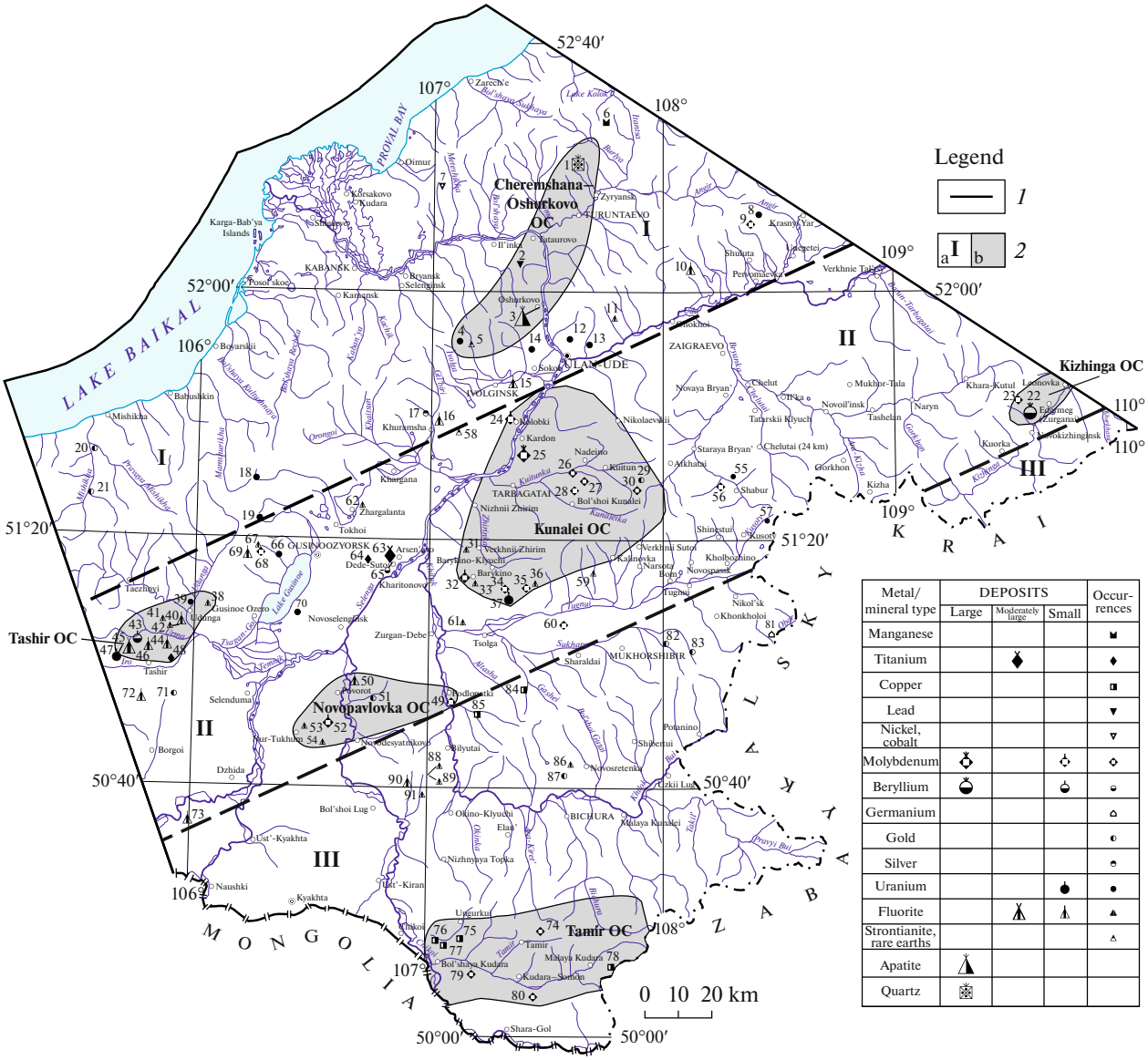


**Fig. 2.** Sketch map of structural–minerogenic zoning and location of ore clusters, deposits, and occurrences in Selenga ore district. map was compiled on basis of geological mapping and topical survey data of Buryatian Geological Administration with authors' amendments and additions. (*1*) Boundaries of Selenga ore district; (*2*) structural–minerogenic zones (a) and ore clusters (b): I, Cisbaikal (Cheremshana–Oshurkovo); II, Selenga–Vitim (Kunalei, Novopavlovka, Kizhinga, Tashir); III, Chikoi–Ingoda (Tamir). Deposits and occurrences: **Zone I:** 1, Cheremshanskoe (lQtz); 2, Lovtsovskoe (oPb); 3, Oshurkovskoe (lAp); 4, Shalutai (oU); 5, Khalyutinskoe (oSr+Ba); 6, Usutaiskoe (oMn); 7, Meteshikhinskoe (oNi, Co); 8, Angyrskoe (Gornoe) (oU); 9, Shibirka (oMo); 10, Pervomaiskoe (sFl); 11, Erkhirikskoe (oFl); 12, Berezovskoe (oU); 13, Udinskoe (oU); 14, Gurul'binskoe (oU); 15, Ivolginskoe (sFl); 16, Tret'yakovskoe (sFl); 17, Malyi Mykert (Sanzhievskoe) (oAg, Pb); 18, Verkhne-Ubukunskoe (oU); 19, Vasil'evskoe (oU); 20, Oseredysh (oAu); 21, Izgib (oAu); **Zone II**: 22, Ermakovskoe (lBe); 23, Zun-Shibirskoe (oMo); 24, Kolobkovskoe (sMo); 25, Zharchikhinskoe (lMo); 26, Nadeinskoe (oMo); 27, Kunalei III (oMo); 28, Kunalei I and II (oMo); 29, Vershinnoe (oAu); 30, Leonovskoe (oMo); 31, Oditsarskoe (oFl); 32, Kharitonovskoe (sMo); 33, Barykinskoe (oFl); 34, Sheno-Baidal (oMo); 35, Shaloty (oMo); 36, Sakhyn-Bulagskoe (oFl); 37, Zhuravlinoe (sU); 38, Galtaiskoe (oFl); 39, Khangaiskoye (oU); 40, Kheltegeiskoe (sFl); 41, Tayozhnoe (oFl); 42, Proyavlenie 6 (oFl); 43, Urminskoe (sU+Be); 44, Ara-Tashirskoe (sFl); 45, Naranskoe (ol); 46, Ubur-Tashirskoe (sFl); 47, Slantsevoe (sU); 48, Iroiskoe (oTi); 49, Podlopatinskoe (oMo); 50, Nizhne-Chikoiskoe (sFl); 51, Virkhe (oAu); 52, Novopavlovskoe (sMo); 53, Shinistuiskoe (oFl); 54, Novopavlovskoe I (oFl); 55, Bryanskoe (oU); 56, Bryanskoe (Koltygeiskoe) (oMo); 57, Kusotinskoe (oU); 58, Arshanskoe (oTR); 59, Nomto-Shibirskoe (oFl); 60, Maysotskoe (oMo); 61, Tsolginskoe (oFl); 62, Manzhinskoe (oFl); 63, Arsent'evskoe (mTi); 64, Verkhne-Zuiskoe (oTi); 65, Sutoiskoe (oBe); 66, Borota (oU); 67, Verkhne-Sanginskoe (oFl); 68, Khambinskoe (oMo); 69, Sharal'dato (sFl); 70, Kholbol'dzhinskoe (oU); 71, Torm' (oAu); 72, Barun–Ul'skoe (sFl); 73, Kharasunskoe (sFl); **Zone III**: 74, Tamirskoe (oMo); 75, Egorovskoe (oCu); 76, Mogoi (oCu); 77, Odinokaya Sosna (oCu); 78, Kudarinskoe (oCu+Mo); 79, Ivanovskoe (Ulan-Ganga) (oMo); 80, Gudzhertuiskoe (oMo); 81, Verkhne-Oborskoe (oGe); 82, Cheremukhovoe (oAu); 83, Saltanovskii prospect (oAu); 84, Altacheiskoe (oCu); 85, Sibil'duiskoe (oCu, Mo); 86, Gochitskoe (oFl); 87, Petropavlovskoe (oAu); 88, Vodorazdel'noe (oFl); 89, Urto-Guinskoe (oFl); 90, Svetlana (sFl); 91, Khol'tskoe (oFl). Deposit and occurrence types and sizes are given in Table 1 and, in parentheses, in figure captions: l, large deposit; m, moderate size deposit; s, small deposit; o, occurrence; OC, ore cluster.

**Table 1.** Structural–minerogenic zoning, deposit types, and undiscovered resources of Selenga ore district

| Geological–genetic type | Ore formation type | Number in map (see Fig. 2) | Deposit (occurrence) name; valuable components | Orebody morphology | Main ore minerals | Reserves, resources | Host lithology/ age | Source |
|---|---|---|---|---|---|---|---|---|
| **Cisbaikal structural–minerogenic zone** | | | | | | | | |
| Cheremshana–Oshurkovo ore cluster | | | | | | | | |
| Metasedimentary | Quartzite | 1 | Cheremshanskoe deposit; silicon | Seams and lenses | Quartz | B, 2397; $C_1$, 10 443; $C_2$, 2275 | Quartzites of Itantsa Formation/Devonian | Ayurzhanaeva and Minina, 2018 |
| Plutonogenic–hydrothermal | Apatite–diorite–gabbro | 3 | Oshurkovskoe deposit; phosphorus | Pockets, veins, veinlets | Apatite | A + B + $C_1$, 108.6 Mt $P_2O_5$ | Gabbroids and diorites of Khalyuta Complex/126–117 Ma | Ripp et al., 2013 |
| Carbonatite | Rare earth | 5 | Khalyutinskoe occurrence; strontium, barium, and rare earths | Sills and dikes | Calcite, barite–celestite, strontianite, magnetite, apatite, phlogopite | $P_1$ + $P_2$ + $P_3$: 11.1 Mt Sr, 9.9 Mt Ba, 275 kt TR | Carbonatites of Khalyuta Complex/130 ± 1 Ma | Ripp et al., 2009 |
| Plutonogenic–hydrothermal | Quartz–gold | 16 | Tret'yakovskoe polymetal ore deposit; gold, silver, fluorite | Veins, silicification zones, stockworks | Molybdenite, pyrite, arsenopyrite, fluorite, azurite | $P_2$: 3.3 t gold, 7.7 t silver | Diabase porphyry dikes and biotite syenites of Bichura Complex | Ivchenko, 1968unp |
| **Selenga–Vitim structural–minerogenic zone** | | | | | | | | |
| Kizhinga ore cluster | | | | | | | | |
| Plutonogenic–hydrothermal | Bertrandite–phenakite–fluorite | 22 | Ermakovskoe deposit; beryllium | Stratiform ledges, stockworks | Bertrandite, phenakite, leucophane, fluorite | $C_2$: 19985 t BeO and 362 kt $CaF_2$ | Alkali granites and syenites of Sogota dike complex and Late Kunalei Complex/226 and 227 ± 1.5 Ma | Lykhin and Yarmolyuk, 2015 |

**Table 1.** (Contd.)

| Geological–genetic type | Ore formation type | Number in map (see Fig. 2) | Deposit (occurrence) name; valuable components | Orebody morphology | Main ore minerals | Reserves, resources | Host lithology/ age | Source |
|---|---|---|---|---|---|---|---|---|
| | | | | Kunalei ore cluster | | | | |
| Plutonogenic–hydrothermal | Porphyry molybdenum | 24 | Kolobkovskoe deposit; molybdenum | Stockwork | Molybdenite, pyrite, magnetite, hematite, fluorite | $C_1$, 20 kt<br>$P_1$, 8 kt | Granites of Sogota Complex | Platov et al., 2000unp |
| Plutonogenic hydrothermal | Porphyry molybdenum | 25 | Zharchikhinskoe deposit; molybdenum | Veinlets, fine dissemination in cement of breccias | Molybdenite, pyrite, and fluorite | $C_1$+$C_2$,<br>61.2 kt Mo total | Leucogranites, porphyry granites, quartz syenites with basites of Bichura, Kunalei, and Sogota complexes/285–286 Ma | Khubanov et al., 2016 |
| Plutonogenic hydrothermal | Porphyry molybdenum | 26 | Nadeinskoe occurrence; molybdenum | Stockwork | Molybdenite | $P_1$, 58 kt | Aureole of porphyry granites with granites of Sogota Complex | Karbainov et al., 1979unp |
| Plutonogenic hydrothermal | Porphyry molybdenum | 32 | Kharitonovskoe deposit; molybdenum | Stockwork | Molybdenite, chalcopyrite, sphalerite, galena, scheelite | $P_1$: 82 Mt ore,<br>55 kt molybdenum | Leucogranites, porphyry granites, and automagmatic breccias of Sogota Complex/194–195 Ma | Khubanov et al., 2016 |
| | | | | Tashir ore cluster | | | | |
| Greisen | Bertrandite–phenakite–fluorite | 43 | Urminskoe deposit; beryllium | Veins, lenses | Helvine, bertrandite | $P_1$, 9 kt | Peralkaline granitoids of Tashir complex | Lykhin and Yarmolyuk, 2014 |
| Veiny epithermal | Fluorite–quartz | 45 | Naranskoe deposit; fluorite | Veins and mineralized crush zones | Fluorite | A + B + $C_1$,<br>1621 kt | Granitoids of Tashir Complex | Bulnaev, 1995 |

**Table 1.** (Contd.)

| Geological–genetic type | Ore formation type | Number in map (see Fig. 2) | Deposit (occurrence) name; valuable components | Orebody morphology | Main ore minerals | Reserves, resources | Host lithology/ age | Source |
|---|---|---|---|---|---|---|---|---|
| | | | Novopavlovka ore cluster | | | | | |
| Plutonogenic hydrothermal | Porphyry molybdenum | 52 | Novopavlovskoe deposit; molybdenum | Stockwork | Molybdenite | $P_1$, 57 kt | Porphyry granites of Sogota Complex | Leshukov et al., 1960unp |
| Liquation | Apatite–titanomagnetite | 63 | Arsent'evskoe deposit; titanium | Lenses, veins | Magnetite, ilmenite | 299207 kt | First-phase gabbro of Bichura Complex 279 ± 2 Ma | Badmatsyrenova et al., 2011 |
| | | | **Chikoi–Ingoda structural–minerogenic zone** | | | | | |
| | | | Tamir ore cluster | | | | | |
| Plutonogenic hydrothermal | Molybdenum–quartz–greisen | 74 | Tamirskoe occurrence; molybdenum | Veins, veinlets | Molybdenite, pyrite, hubnerite, rutile | $P_2$, 185 kt | Dikes of Ust'-Tamir subvolcanic complex in granitoids of Bichura Complex | Kuznetsova, 1973unp |
| Plutonogenic hydrothermal | Molybdenum–quartz–greisen | 79 | Ivanovskoe occurrence, molybdenum | Stockwork | Molybdenite, pyrite, chalcopyrite, wolframite | $P_1$, 177 kt | Ust'-Tamir subvolcanic complex, $T_{2-3}$ | Koshkin et al., 2000unp |
| Plutonogenic hydrothermal | Porphyry molybdenum–copper | 78 | Kudarinskoe occurrence, copper and molybdenum | Stockwork | Molybdenite, chalcopyrite, pyrite, ilmenite, rutile | $P_1$: 3087 kt copper, 52 kt molybdenum | Granitoids of Bichura Complex | Efimov, 2010 |

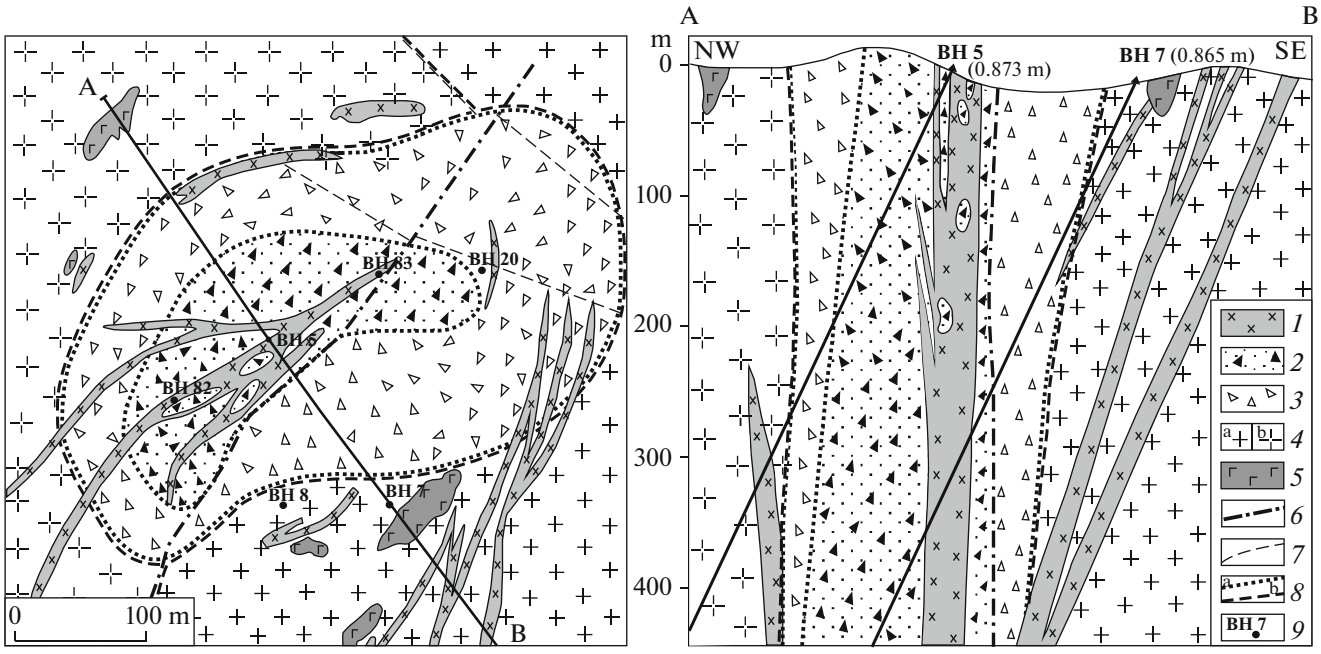


**Fig. 3.** Geological sketch map of Zharchikhinskoe molybdenum deposit and exploratory cross section A–B. After (Vernik et al., 1983unp) with authors' additions and amendments. (*1–3*) Sogota subvolcanic complex, Middle–Late Triassic: (*1*) Ore-bearing porphyritic granite and porphyry granite dikes; (*2*) essentially polymictic eruptive breccias of granites, quartz syenites, and albitized syenites with trachyrhyolite, trachyte, and microsyenite dikes; (*3*) monomictic explosive breccias of K-feldspathized granosyenites and syenites; (*4*) granitoids of (a) Early Permian Bichura complex (leucogranites, porphyritic granites, quartz syenites); (b) Late Permian–Early Triassic Kunalei Complex (subalkaline and alkaline granites and syenites); (*5*) xenoliths of first-phase monzonites and diorites of Bichura Complex; (*6*) axial fault line; (*7*) other faults; (*8*) conventional boundaries of areal extent of explosive breccias of Zharchikinskaya ring structure (a); granitoids of Bichura and Kunalei complexes (b); (*9*) borehole and its number. BH, borehole.

prospecting and exploration operations, followed by geological–structural, petrological–geochemical, and environmental surveys (Vernik et al., 1983unp; Vernik and Tantsyrev, 1990unp; Gusev et al., 2008unp). A detailed description of this deposit is available in the published literature (Pokalov et al., 1985; Ignatovich and Fil'ko, 1978; Skripkina et al., 1982; Vernik and Ripp, 1995; Ignatovich, 2007; etc. (Fig. 3).

The deposit is composed largely of intrusive rocks of the Bichura Complex (leucogranites, porphyry granites, quartz syenites, and basites) with a U–Pb zircon age of 285–286 Ma (Khubanov et al., 2017) and the Late Permian–Early Triassic Kunalei Complex (subalkaline and alkaline granites and syenites that crosscut Upper Permian volcanics of the Alentui Formation (trachytes, trachyrhyolites, ignimbrites, trachybasaltic andesites, and tuffs of respective compositions).

These were followed by emplacement of Middle–Late Triassic intrusions of subalkaline leucocratic granites and syenites of the Late Kunalei Complex and the porphyry granites of the Sogota subvolcanic complex. The Zharchikhinskaya ore-bearing explosive structure formed during the latest Triassic.

This structure is a concentrically zoned body of polymictic and monomictic breccias with circular and conical dikes associated with the breccia body. The body was formed in three stages, (1) essentially monomictic explosive K-feldspathized granosyenite and syenite breccias; (2) peripheral wallrock breccias; trachyrhyolite, trachyte, and microsyenite dikes; (3) essentially polymictic eruptive granite, quartz syenite, and albitized syenite breccias. The surface outcrop of the ore-bearing brecciated rocks is ovate, measures 670 × 300 m, and extends northeastward. According to drilling data, the ore-bearing breccias extend downward as deep as 800 m. This tubular structure is distinctly confined to a junction of differently oriented faults. Dikes account for up to 15% of the total volume of the breccia body. The dikes are mostly granite and syenite. Most dikes are oriented northeastward. The dikes are predominantly preore. The earliest of them are composed of microsyenites, microgranosyenites, and trachyrhyolites. Porphyritic granite, rhyolite, and pegmatite dikes formed later. Thin alkali granite dikes were also identified, which were emplaced after molybdenum-bearing, quartz–fluorite, and quartz–pyrite veinlets.

The deposit is represented by the almost vertical tubular body of mineralized eruptive breccias of the

**Table 2.** Reserves and undiscovered resources of Zharchikhinskoe molybdenum deposit (Platov et al., 2009).

| Reserves and resources | Mo ore, Mt | $Mo_{total}$, kt/cont., % | $Mo_{sulf.}$, kt/cont., % | OMR | Pyrite sulfur, Mt/cont., % | $CaF_2$, Mt/cont., % |
|---|---|---|---|---|---|---|
| $C_1+C_2$-category reserves | | 61.2/0.091 | 56.1/0.08 | 0.76 | | |
| Uneconomic reserves | | 19.6/0.085 | 18.3/0.08 | 0.63 | | |
| $P_1$-category resources | 60 | 50/0.078 | 48.1/0.078 | | 1.2/0.6 | 1.4/1.52 |

Sulf, sulfide; cont., content; OMR, ore mineralization ratio (ratio between net ore volume and total orebody volume).

Sogota Complex. The orebody virtually coincides with the breccia body. The mineralization is represented by molybdenite, pyrite, and fluorite. Molybdenite is concentrated in molybdenite–quartz and molybdenite veinlets and also occurs as fine disseminations in the breccia cement. Its content in the stockwork varies from a few thousandths to 1%; the average grade is 0.088%. The fluorite content in the orebody varies from several tenths to 2–5%, rarely higher. In general, fluorite is ubiquitous at the deposit. An increase in fluorite content has been recorded in zones of elevated beryllium content. The presence of fluorite–phenakite–bertrandite-type beryllium mineralization is a characteristic feature of this deposit. Beryllium is unevenly distributed at the deposit. The bulk of it was deposited during the preore stage. The deposit has been thoroughly explored. Reserve and undiscovered resource estimates are given in Table 2.

It should be noted that approximately 30% of reserves are rich ores with a Mo grade of 0.153%. Moreover, drilling data indicate an increase up to 0.5% in the Mo concentration at a depth of 400–600 m. Conditions are favorable for opencast mining at the deposit. Up to 91% of molybdenum can be recovered by hydrometallurgical concentration of primary ores and up to 70–80% by in-situ leaching of oxidized ores. The deposit is ready for mining, but it remains shut down at the moment (Platov et al., 2009; Bakhtin et al., 2007).

*The Kharitonovskoe molybdenum deposit* was discovered as a result of 1 : 50000 geological mapping (Karbainov et al., 1979unp). It is confined to a stock of leucogranites, porphyry granites, and automagmatic breccias of the Middle–Upper Triassic–Early Jurassic Sogota complex (Fig. 4).

The U–Pb zircon age of the leucogranites of the Sogota Complex is 194–195 Ma (Khubanov et al., 2017). They crosscut alkali granites and syenites of the Late Kunalei Complex with a radiometric age of 230–229 Ma (Reichow et al., 2010; Khubanov et al., 2017). The stockwork measures 800 × 1100 m in plan view and has been confirmed downward to a depth of more than 500 m. The zone of richest mineralization in the stockwork coincides with the outline of the magmatic breccia body (Izvekov et al., 1972unp) and measures 400 × 700 m on the surface. The oxidation zone of the deposit extends downward as deep as 6–70 m (Ignatovich and Fil'ko, 1978).

The stockwork consists of quartz–molybdenite, molybdenite, pyrite, and quartz–pyrite veinlets. The veinlets were found to contain chalcopyrite, sphalerite, galena, and scheelite in small amounts. Veinlet density varies; four orebodies have been recognized. They are located along the southern contact of the granite–porphyry stock. The first body is characterized by a strike length of presumably 760 m; dip length, more than 500 m; thickness, 9.3 m; average molybdenum grade, 0.053%; and ore mineralization ratio (OMR) of 1.0. The second body has lengths of 360 and 550 m, respectively; thicknesses of 58.9–76.6 m; Mo grade of 0.043%; and OMR of 0.26–0.43. The third body has lengths of 730 and 800 m; a thickness of 86.7–137.7 m; Mo grade of 0.062%; and OMR of 1.0. The fourth has the lengths of 860 and 760 m; a thickness of 53.4 m; Mo grade of 0.052%; and OMR of 0.34 to 1.0 (Ignatovich, 2007). The ores contain scheelite (tungsten trioxide content is 0.03–0.04%). The molybdenum grade values mentioned above are underestimated because of the established high values of selective core grinding while drilling. For this reason, the geologists could not classify part of the deposit's reserves explored in most detail as category $C_2$. However, considering that the actual ore grade is much higher than that estimated from the faulty core sampling data, as well as the geographically and economically favorable location of the deposit, there are grounds for undiscovered resources that may meet the required conditions. Therefore, it is necessary to undertake additional studies of the actual molybdenum grade in the ores (Koshkin et al., 1999unp).

*The Kolobkovskoe molybdenum deposit* has been covered by preliminary exploration surveys (Barskii and Koledenko, 1981unp). The deposit is a linear N–S trending stockwork zone in the domain of the Middle–Upper Triassic granites of the Sogota Complex (Fig. 5). The stockwork zone measures 1000 × 50 m in plan view and has been confirmed downward to a depth of 400 m. The ore mineralization consists of molybdenite, pyrite, magnetite, hematite, and fluorite. Wallrock alteration is represented by pyritization, chloritization, and epidotization. Molybdenum reserve estimates are given in Table 2. Conditions are favorable for opencast mining (Platov et al., 2000unp).

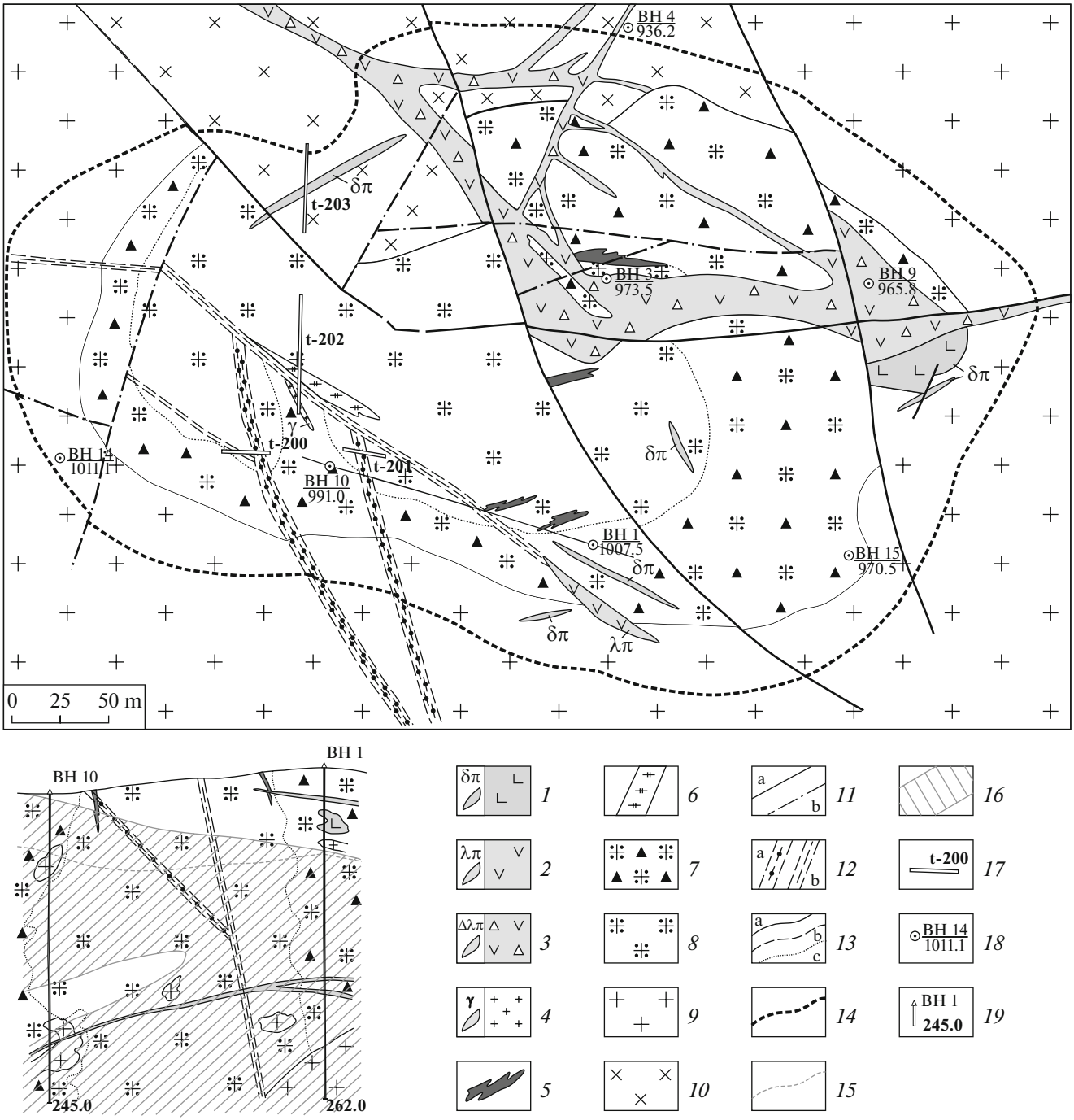


**Fig. 4.** Geological sketch map of Kharitonovskoe molybdenum deposit and exploratory cross section along row of boreholes 1–10. Modified after Barskaya et al., (1984unp). (*1–8*) Sogota subvolcanic complex, Middle–Upper Triassic–Early Jurassic: (*1*) Diorite porphyries; (*2*) porphyritic andesites; (*3*) automagmatic breccias of porphyritic andesites; (*4*) fine-grained leucogranites; (*5*) quartz veins; (*6*) pegmatite veins; (*7*) eruptive breccias of porphyry granites; (*8*) porphyry granites; (*9–10*) Late Kunalei Complex, Late Permian: (*9*) medium- to fine-grained granites, (*10*) medium-grained syenites; (*11*) faults: (a) proven, (b) inferred; (*12*) zones of cataclasis (a) and mylonitization (b); (*13*) geological boundaries: (a) proven, (b) inferred, (c) between various facies; (*14*) boundary of extensive stockwork-type silicification zone; (*15*) boundary of oxidation zone; (*16*) orebodies with Mo content higher than 0.03%; (*17*) trench lines; (*18*) boreholes and their numbers; (*19*) borehole, its number, and depth in cross section. t, trench; BH, borehole.

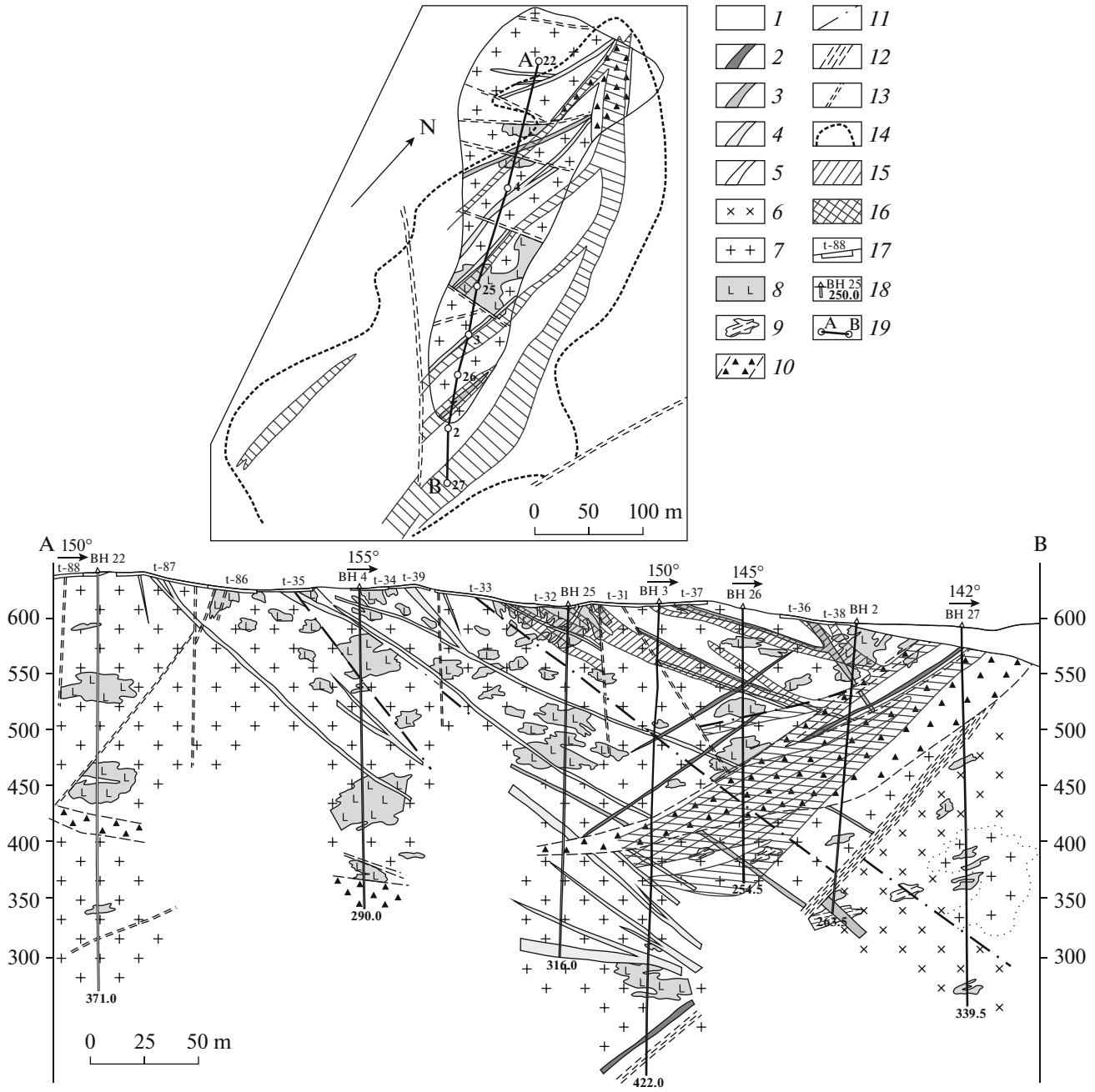


**Fig. 5.** Geological sketch map of Kolobkovskoe molybdenum deposit and exploratory cross section A–B. After Barskii and Kolodenko, (1981unp) with amendments and additions. (*1*) Loose Quaternary sediments; (*2–5*) Sogota subvolcanic complex: (*2*) porphyry diorite dikes; (*3*) felsite and porphyritic felsite dikes; (*4*) porphyry syenite dikes; (*5*) fine-grained granite and porphyry granite dikes and small stocks; (*6–7*) Kunalei intrusive complex, Late Permian–Early Triassic: (*6*) leucocratic syenites, (*7*) porphyritic granites; (*8*) biotite diorites and monzonites of Bichura Complex, Early Permian; (*9*) Precambrian biotite–pyroxene–plagioclase hornfelses and hornfelsed biotite shales; (*10*) tectonic breccias; (*11*) mylonitization and brecciation zones; (*12*) crush and cataclasis zones; (*13*) faults; (*14*) primary halo with Mo content higher than 0.001%; (*15*) orebodies with Mo content higher than 0.03%; (*16*) orebodies with Mo content higher than 0.1%; (*17*) trench and its number; (*18*) borehole and its number and depth; (*19*) exploratory section line. t, trench; BH, borehole.

A number of large molybdenum occurrences have been discovered in the Kunalei ore cluster that can be upgraded to the status of deposits after necessary additional surveys. These include, first, the Leonovskoe and Nadeinskoe prospects. *The Leonovskoe molybdenum occurrence* is confined to the contact of the Middle–Upper Triassic porphyry granites of the Sogota Complex with the Upper Permian rocks of the Alentui Formation. The nearly isometric stockwork measures 170 × 175 m in plan view and has been confirmed

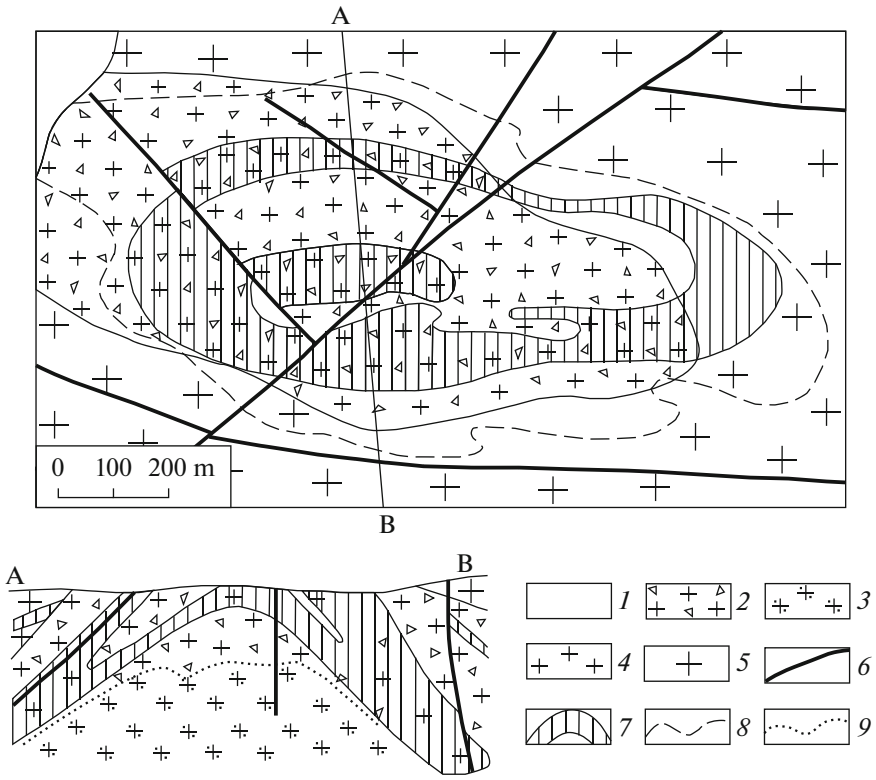


**Fig. 6.** Geological sketch map and cross section A–B of Novopavlovskoe deposit. After Baturina and Ripp (1984) with additions (*1*) Quaternary sediments; (*2–4*) Sogota subvolcanic complex, Middle–Late Triassic: (*2*) eruptive breccias of porphyry granites, (*3*) porphyritic granites and porphyry granites, (*4*) fine-grained leucocratic granites; (*5*) subalkaline granites, granosyenites, syenites, and quartz syenites of Kunalei intrusive complex, Late Permian–Early Triassic; (*6*) faults; (*7*) ore ledge; (*8*) outlines of endogenic molybdenum halo; (*9*) inferred geological boundary between porphyry granites and eruptive breccias.

downward to a depth of 300 m. The ore mineralization consists of molybdenite, pyrite, chalcopyrite, galena, and fluorite. Molybdenite is concentrated in molybdenite–quartz veinlets and sometimes occurs as disseminations. Undiscovered category $P_1$ resources are estimated at 4.05 kt molybdenum in ores with an average grade of 0.071%. The Leonovskoe ore occurrence compares well in ore quality with the Zharchikhinskoe and Kolobkovskoe deposits (Barskaya et al., 1984unp; Platov et al., 2000unp). *The Nadeinskoe molybdenum occurrence* has been covered by prospecting surveys (Karbainov et al., 1979unp). It is confined to the endo- and exomorphic contacts of the porphyry granites and granites of the Middle–Upper Triassic Sogota Complex. The deposit is a stockwork measuring 1500 × 1200 m in plan view and has been confirmed downward to a depth of 130 m. Two orebodies have been recognized from sampling data. The first (upper) is largely eroded. Its mineralization is represented by flaky molybdenite dissemination and, sometimes, molybdenite and molybdenite–quartz veinlets. The second (lower) orebody concentrates the bulk of ore resources of this occurrence. It measures 900 × 600 m in plan view. The ore stockwork consists of molybdenite–quartz, molybdenite–pyrite–quartz, and molybdenite veinlets, sometimes disseminated molybdenite. Undiscovered $P_1$-category resources are estimated at 58 kt molybdenum in ores with an average grade of 0.066% and OMR of 0.77. In spite of the low molybdenum content in ores, the Nadeinskoe ore occurrence is twice as large as the Kolobkovskoe deposit in terms of undiscovered resource volume (Platov et al., 2000unp).

The Novopavlovka ore cluster includes the discovered and explored Novopavlovskoe molybdenum deposit and the Podlopatinskoe occurrence, as well as a number of other fluorite and gold prospects (Leshukov et al., 1960unp).

*The Novopavlovskoye deposit* is confined to a Middle–Late Triassic granite porphyry stock of the Sogota Complex (Leshukov et al., 1960unp; Karbainov et al., 1977unp; Baturina and Ripp, 1984). The stock is mapped on the surface as a northeast trending ovate body that measures 1 × 0.5 km and consists of hydrothermally altered porphyry granites and fine-grained leucogranites (Fig. 6).

The deposit is classified as plutonogenic–hydrothermal and represented by the surface outcrop of a ledge of economic molybdenum ores associated with a porphyry granite stock. In plan view, the ledge is shaped as a closed ring 30–180 m in width, which dips

away from the center, resembling a symmetrical anticline. Its thickness is 70–100 m. Two orebodies (upper and lower) have been recognized within the ledge. They occur as steeply dipping (35°–55°) strips of ore-bearing rocks separated by a 50- to 70-m-thick barren interval. The maximum ore intersection depth is 290 m. The ore mineralization is confined to strongly fractured and crushed rocks; the molybdenum grade varies from 0.012 to 0.28%. Molybdenum ores are predominantly disseminated, but ore veinlets have also been encountered. The richest ores with molybdenum grades up to 0.2–1% are associated with quartz–molybdenite and quartz–molybdenite–pyrite veinlets. The combined proportion of such ores does not exceed 5–7%. The undiscovered category $P_1$ resources were estimated only for the lower orebody at 57 kt in ROM and lean ores including 18 kt in rich ores (Koshkin et al., 2002unp).

The prospective Tamir ore cluster with the Tamirskoe, Ivanovskoe, and Kudarinskoe large molybdenum and copper–molybdenum occurrences has been recognized in the Chikoi–Ingoda structural–minerogenic zone.

*The Tamirskoe molybdenum occurrence* is morphologically classified as veiny. It is located within the areal extent of the Permian medium-grained biotite granitoids of the Bichura intrusive complex (Yablokov et al., 1955unp; Novikov et al., 1973unp). The Middle–Late Triassic porphyry granite and, sometimes, aplite-like granite dikes are widespread within the occurrence and occupy ~30% of its area. The dikes are characterized by continuous sublatitudinal orientation. The dip angles of the dikes are, as a rule, close to vertical (80°–90°). Their lengths vary widely from 30 to 500 m, and thicknesses, from a few centimeters to 6 m. The porphyry granite dikes are spatially associated with quartz veins bearing molybdenum mineralization. In addition to molybdenite, the quartz veins contain pyrite, hubnerite, and rutile in small amounts and gangue minerals—beryl, tourmaline, and muscovite. The quartz veins make up three vein zones—western, eastern, and central, separated by ~150-m-wide intervals (Fig. 7).

Veins within the zones are close to each other and arranged en echelon. The veins are 0.1–0.3 m in thickness and 30–40 m in length; some veins extend as far as 50–150 m. The strike of the veins is sublatitudinal; the dip is northward. Vein-filling quartz is milky white or light gray; fine- to medium-grained, sometimes coarsely crystalline; it is represented by one generation and classified as a high-temperature variety. Molybdenite is finely flaky; it fills pockets and veinlets in vein selvages and is partially oxidized to Fe-molybdite. Wallrocks are greisenized near quartz veins (10–20 cm); molybdenite within them occurs as fine disseminations. The molybdenum content varies from 0.003 to 0.3%. Undiscovered category $P_2$ molybdenum resources are estimated at 185 kt (Koshkin et al., 2000unp). In our opinion, the large Tamir molybdenum ore occurrence requires further detailed exploration and additional studies with the objective of upgrade to a deposit.

*The Ivanovskoe molybdenum occurrence* is represented by a quartz–molybdenite stockwork hosted by the Upper Permian bimodal basalt–rhyolite volcanics of the Tamir Formation. The latter are also crosscut by Middle–Late Triassic microdiorite, porphyry diorite, and porphyry granite dikes of the Ust'-Tamir subvolcanic complex (Gordienko, 1980). The ore control is the Chikoi–Kudara fault zone. The E–W trending ovate stockwork has an area of 2.7 km$^2$. It consists of a core with an area of 1.5 km$^2$ and an average molybdenum grade of up to 0.05%, surrounded by vein and veinlet (stockwork) zones with molybdenum grades up to 0.03% (Yablokov et al., 1955unp). Several 6–250 m thick ore zones with molybdenum grade of 0.03–0.05% have been recognized at depth. Mineral composition of veinlets is as follows: quartz; potassium feldspar; tourmaline, beryl, muscovite, and fluorite in small amounts; ore minerals: molybdenite, pyrite, chalcopyrite, hematite, magnetite, wolframite, scheelite, galena, sphalerite, chalcocite, powellite, stannite, covellite, cinnabar, tennantite, tetrahedrite, and bismuthite. Secondary wallrock alterations: K-feldspathization, berezitization, and secondary quartzites. Metal distribution in primary halos suggests that the molybdenum occurrence formed above the intrusion and its erosional truncation is insignificant. The undiscovered category $P_1$ molybdenum resources are estimated at 177 kt (Koshkin et al., 2000unp).

*The Kudarinskoe copper–molybdenum ore occurrence* is stockwork-type. It is located in the axial part of the Kudara Esker in the Chikoi–Kudara fault zone (Novikov et al., 1973unp; Efimov, 2010). The main ore field is composed of Upper Permian gabbros and granitoids of the Bichura complex, which include xenoliths of Neoproterozoic schists of the Kataevo Formation and acid volcaniclastics of the Tamir Formation ($P_2$). The granitoids of the Bichura Complex are crosscut by porphyry granite dikes and small stocks of the Ust'–Tamir subvolcanic complex at the intersections of E–W trending major faults with a N–S fault in the central part of the prospect. The ore occurrence is confined to the granitoid stocks: two ore-bearing stockworks, the Northern and Southern, have been delineated in their apical parts.

The Northern stockwork is curvilinear, roundish, and slightly elongate in northeastward direction and measures 1300 × 800 m. The lower boundary is located at a depth of 280 m. The Southern stockwork (500 × 200 m) is located 1.5 km south of the Northern. The rocks within stockworks are silicified, albitized, locally K-feldspathized, biotitized, and strongly greisenized. The ore mineralizaion is represented by primary and secondary vein–disseminated ores that

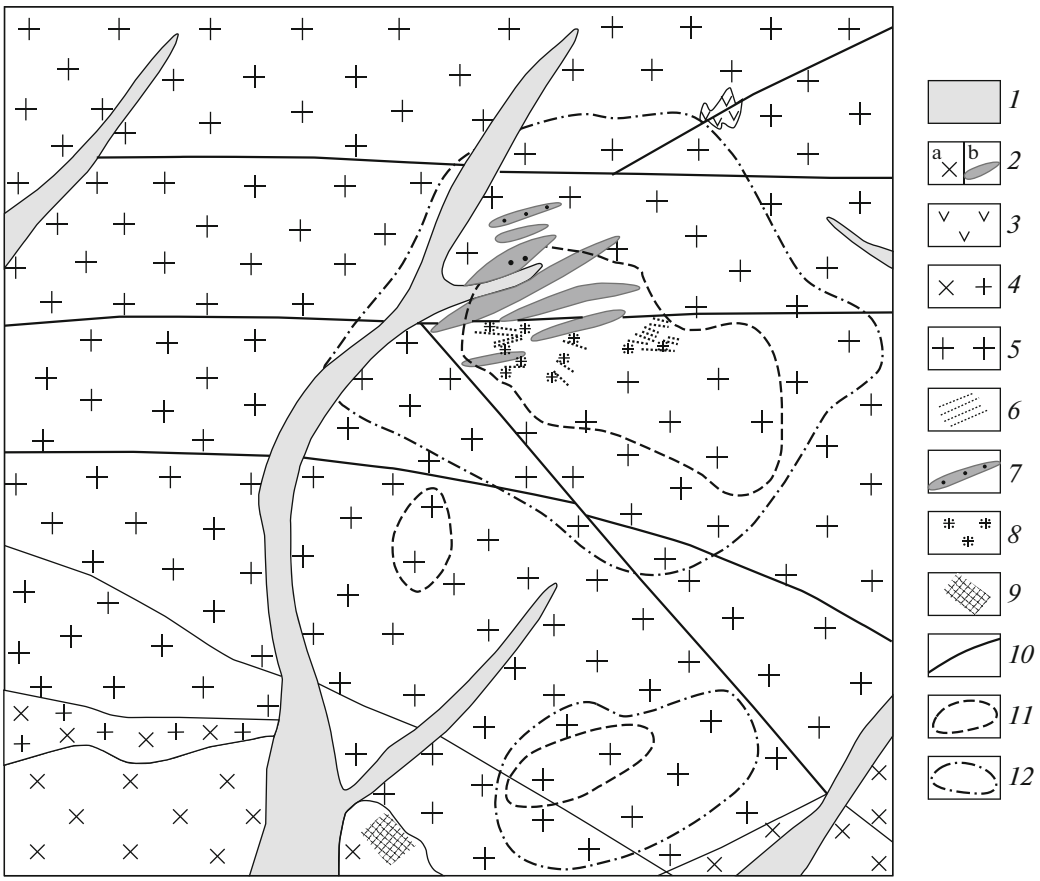


**Fig. 7.** Geological sketch map of Tamirskoe molybdenum occurrence at 1 : 10000 scale. After (Novikov et al., 1973unp and Kuznetsova, 1973unp), with additions and amendments. (*1*) Quaternary sediments; (*2–3*) Ust'–Tamir subvolcanic complex, Middle–Upper Triassic: (*2*) stocks and dikes of porphyry syenites (a) and porphyry granites (b); (*3*) trachyrhyolite and andesite clastolavas of Tamir Formation, Upper Permian; (*4–5*) Bichura intrusive complex, Permian: (*4*) fine-grained biotite granosyenites (apical facies), (*5*) medium-grained biotite and biotite–hornblende granites; (*6*) quartz veins with molybdenite; (*7*) molybdenite dissemination in porphyry granites; (*8*) greisenization; (*9*) argillization; (*10*) faults; (*11–12*) molybdenite halos: (*11*) primary (up to 0.3%), (*12*) secondary (up to 0.001%).

occur mostly in the central part of the Northern ore-bearing stockwork (Fig. 8).

Weakly mineralized rocks with mostly veinlet-type mineralization have been reported at the peripheries of the ore-bearing stockworks within the main ore-controlling structures and primary halos. The main ore minerals of the primary ore zone are molybdenite, chalcopyrite (1–2%), pyrite (1–3%), ilmenite (up to 1%), and rutile (up to 1%); magnetite, hematite, chalcocite, bornite, covellite, sphalerite, and galena are less frequent. Major gangue minerals are quartz, feldspar, and sericite, which account for 90–95 wt % of the ore. Silver (up to 1 g/t) and gold (0.05–0.1 g/t) occur as by-products. The primary ores are essentially chalcopyrite, disseminated and vein–disseminated; the average copper content is 0.3%; the molybdenum content, 0.01%. The undiscovered resource estimates for the Kudarinskoe ore occurrence are given in Table 1. Genetically, it has been attributed to the prospective porphyry copper formation and correlated with the Erdenetuin-Obo deposit in northern Mongolia (Efimov, 2010). In our opinion, the Kudarinskoe ore occurrence, represented by two large stockworks, requires further detailed studies and upgrading to the status of a rich polymetal ore deposit.

**Beryllium.** The Ermakovskoe beryllium deposit in the Selenga ore district is unique in terms of strategic mineral resources. It was discovered by G.A. Ermakov in 1964 as a result of 1 : 200000 mapping surveys in the northwestern part of the Mesozoic Kizhinga Depression. Later, after detailed exploration, the scientific work of researchers of the Fedorovskii Scientific Research Institute of Mineral Resources (VIMS), the Institute of Geology of Ore Deposits, Petrography, Mineralogy, and Geochemistry (IGEM) of the Russian Academy of Sciences, the Geological Institute of the Siberian Branch of the Russian Academy of Sciences, and other organizations have played a significant role in the petrological–geochemical studies and commercial assessment of this unique deposit and the adjacent territory of Western Transbaikalia. As a result, the large West Transbaikalian beryllium-

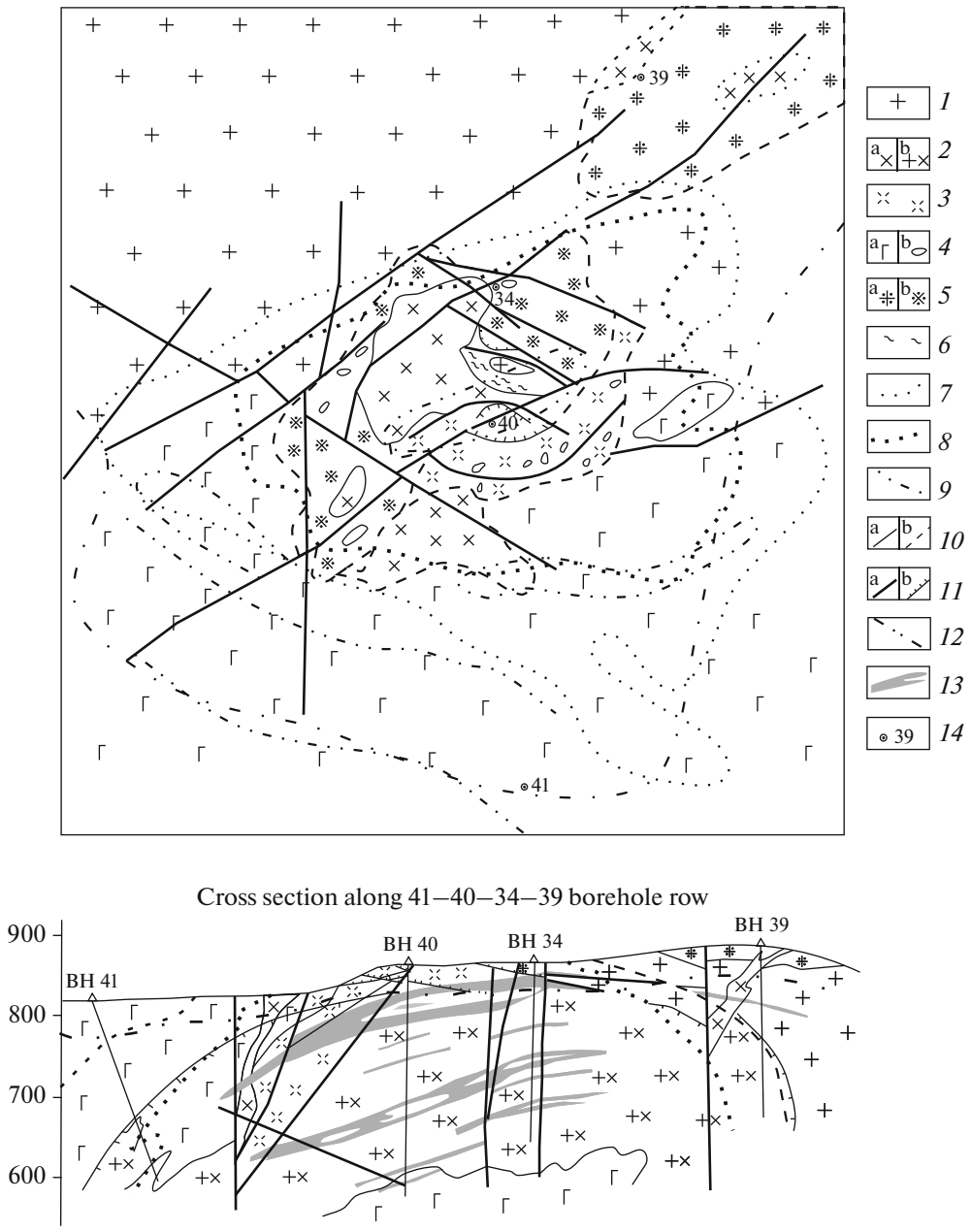


**Fig. 8.** Geological sketch map of Northern stock of Kudarinskoe copper–molybdenum ore occurrence at 1 : 2000 scale and cross section along 41–40–34–39 borehole row. After (Efimov, 2010) with additions and amendments. (*1–2*) Ust'–Tamir subvolcanic complex, Middle–Upper Triassic: (*1*) granites, porphyry granites, quartz porphyries; (*2*) plagiogranites (a), quartz diorites and syenodiorites (b); (*3–4*) Bichura intrusive complex, Upper Permian: (*3*) granodiorites, (*4*) gabbrodiorites (a) and diorites (b); (*5*) greisenized granitoid varieties (a) and quartz–muscovite greisens (b); (*6*) crush and foliation zones; (*7*) primary halos with 0.03–0.09% copper; (*8*) ore-bearing basic rocks with copper content of 0.1–0.3%; (*9*) outlines of stock of altered ore-bearing rocks based on magnetic data; (*10*) intrusive contacts: proven (a) and inferred (b); (*11*) faults: high-angle (a) and low-angle (b); (*12*) primary halo with molybdenum content up to 0.01%; (*13*) ore-bearing stockwork rocks with 0.3–0.6% copper; (*14*) boreholes and their numbers. BH, borehole.

bearing province was recognized within the regional Selenga–Vitim metallogenic belt. The published monographs and numerous papers on a comprehensive description of the Ermakovskoe and other beryllium deposits in the West Transbaikalian province (Ginzburg et al., 1969; Ripp, 1995; Bulnaev, 1996; Kovalenko et al., 2003; Lykhin et al., 2004; Kupriyanova et al., 2009; Kupriyanova and Shpanov, 2011; Lykhin and Yarmolyuk, 2015; etc.) obviate the need for detailed descriptions of these thoroughly studied deposits.

The Kizhinga ore cluster is located in the southeastern part of the Selenga ore district within the

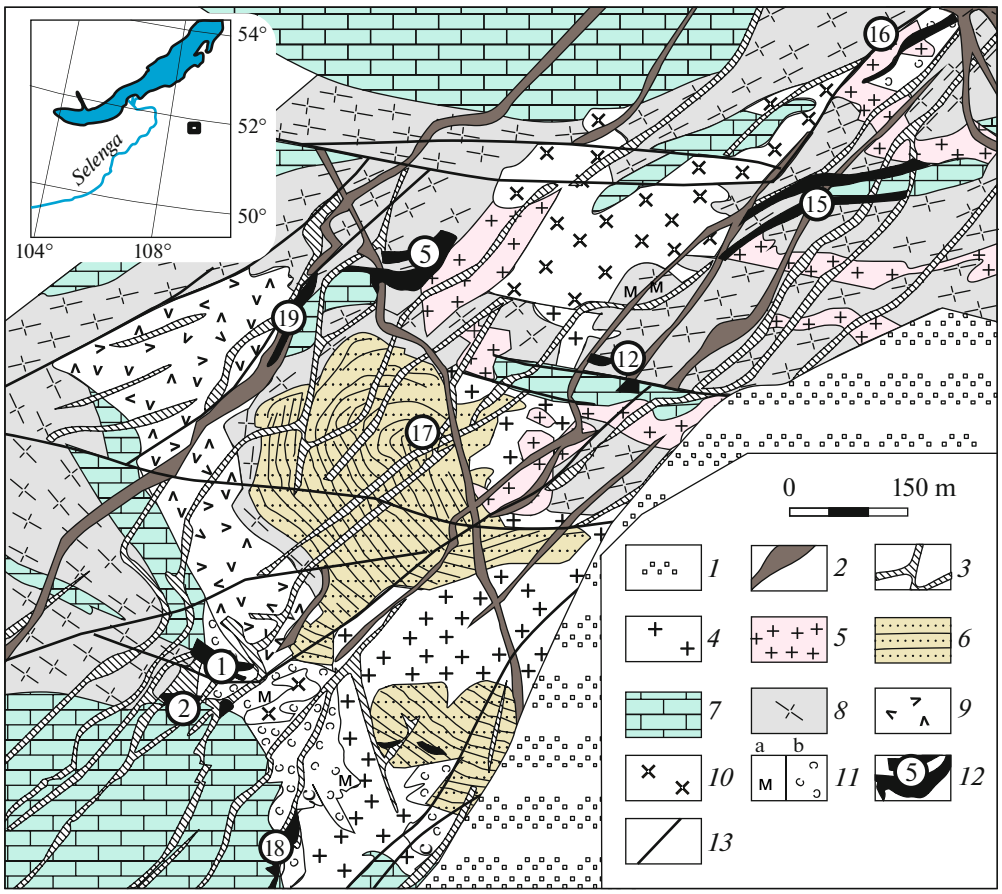


**Fig. 9.** Geological sketch map of Ermakovskoe deposit. After (Gal'chenko et al., 1968unp). (*1*) Cretaceous sediments (conglomerates, gravelites, sandstones); (*2–5*) Sogota dike and Late Kunalei intrusive complexes, Late Permian–Late Triassic: (*2*) porphyry felsite and porphyry syenite dikes, (*3*) syenodiorite and porphyry diorite dikes, (*4*) leucocratic subalkaline granites and quartz syenites, (*5*) fine-grained leucocratic granites; (*6–7*) Neoproterozoic metasedimentary rocks: (*6*) sandstones interbedded with limestones and shales, (*7*) dolomites; (*8–10*) intrusive rocks of Zaza Complex, Middle–Late Carboniferous–Early Permian: (*8*) granites and granodiorites, (*9*) gabbro and gabbrodiorites, (*10*) quartz syenites; (*11*) microclinites (a) and vesuvianite–garnet–diopside skarns (b); (*12*) ore zones (numerals in circles); (*13*) faults.

northeast trending Kizhinga–Kudun metallogenic zone (170–180 km long with a maximum width of 20 km), where two unique beryllium deposits, Ermakovskoe phenakite–bertrandite–fluorite and Orotskoe bertrandite, have been explored.

*The Ermakovskoe phenakite–bertrandite–fluorite deposit* is located on the northwestern uplifted flank of the Mesozoic Kizhinga rift trough, which is controlled by northeast trending regional faults. According to D.A. Lykhin and V.V. Yarmolyuk (Lykhin and Yarmolyuk, 2015) and exploration data, the deposit is confined to a large xenolith of Neoproterozoic metamorphosed clastic–carbonate–dolomite rocks, which were crosscut by gabbroids (332 ± 1 Ma) and granite dikes and intrusions of the Zaza Complex dated at 325 ± 3, 316 ± 2, and 302.5 ± 10 Ma during the preore stage. Ore mineralization is genetically related to the Sogota dike complex and the Late Kunalei alkali granite and syenite complex with U–Pb ages of 226 Ma (Shtok massif) and 227 ± 1.5 Ma (Sienit massif) (Fig. 9).

The Ermakovskoe deposit is attributed to the bertrandite–phenakite ore formation and the economic ore type of bertrandite–phenakite–fluorite metasomatites (Kupriyanova et al., 2009). Twenty-four lenticular orebodies that make up 19 ore zones varying from 20 to 170 m in length and from 0.5 to 23 m in thickness have been recognized at the deposit (see Fig. 9, Table 3). The orebodies are metasomatic ledges and veinlet mineralization zones in skarnified rocks. The major ore minerals are bertrandite, phenakite, and fluorite. Phenakite (which accounts for almost half the BeO reserves of the deposit) occurs as radiated columnar aggregates up to 4 cm in diameter.

Bertrandite makes up fan- and sheaflike aggregates. Fluorite occurs as segregations up to 10 cm across. The ores are multicomponent fluorite–beryllium. The approved category $C_2$ reserve estimates (Table 1) are 19 985 t BeO and 362 kt $CaF_2$. By January 1, 1997, the initial total metal reserves of the deposit had been depleted by 37% as a result of mining

**Table 3.** Positions and parameters of ore zones at Ermakovskoe deposit (after Kupriyanova and Shpanov, 2011)

| Ore zones | Position in fold | Average concentration, wt % | | Reserves, % |
|---|---|---|---|---|
| | | Fluorite | BeO | |
| 1 | Southern limb | 24.4 | 1.34 | 66.6 |
| 2 | Southern limb | 8.9 | 0.77 | 4.9 |
| 5 | Northern limb | 26.5 | 1.38 | 5.2 |
| 12 | Northern limb | 26.1 | 1.16 | 10.8 |
| 15 | Northern limb | 22.7 | 0.75 | 2.6 |
| 16 | Northern limb | 22.5 | 0.78 | 2.5 |
| 17 | Flat trough of fold | 18.3 | 0.86 | 6.4 |
| 18 | Northern limb | 29.7 | 0.92 | 0.5 |

(Pekhterev et al., 2012). However, the remaining reserves are sufficient to consider the Ermakovskoe as a world-class economic deposit. At present, the Ermakovskoe is being prepared for further development and commercial mining (Takhanova, 2017).

*The Orotskoe bertrandite deposit* is located 28 km northeast of the Ermakovskoe, at the head of the Orot gorge (Fig. 10). It was discovered in 1977 by N.V. Rivlin and M.V. Kudrin as a result of detailed 1 : 10000 prospecting surveys. The deposit is related to the formation of the Orot central-vent paleovolcano with a distinctly expressed caldera ~4 km in diameter (Gordienko, 1987). The caldera is surrounded by ring fissures that were recognized from aerial images. An irregularly shaped, 800-m-long, N–S trending neck, extending along the eastern edge of the caldera, was formed in a vent and filled with trachyrhyolite lava with numerous wallrock fragments (eruptive breccia). The neck is surrounded by a halo of near-vent wallrock breccia that consists of crushed wallrocks that underwent hydrothermal metasomatic alteration and ore mineralization. The porphyry granite intrusion of the Kunalei Complex is a ring dike, which grades into a semilaccolith on the northeastern side of the caldera, and is confined to the fault that determines the boundary of the laccolith. The dikes fill arcuate fractures.

The Orot paleovolcano formed in several stages. (1) The inception of the paleovolcano, related to the emplacement of coarsely porphyritic syenite and trachyte–trachyrhyolite subvolcanic intrusions; their eruptive contacts with the Early Permian volcanites of the Suzha Formation and the granites of the Kunalei Complex have been repeatedly observed. (2) The formation of an eruptive breccia neck (vent facies); the eruptive breccias contain fragments of first-stage rocks. (3) Emplacement of the porphyry granite ring intrusion, related to the caldera formation process; this is supported by the spatial relationship of the granites and the arcuate faults that bound the caldera. The porphyry granites crosscut the eruptive breccia. (4) Formation of various dikes; the beryllium mineralization is concentrated mostly in porphyritic alkaline (aegirine-bearing) leucocratic granites, which make up a semiring intrusion at the deposit, and in the wallrock breccias and volcanites.

In addition to the vent facies of volcanic rocks, the Orot paleovolcano is surrounded by widespread sheet facies of volcanic rocks of the Alentui ($P_2$) and Suzha ($P_1$) formations, which were later included in the single Tsagan–Khuntei sequence (Late Permian–Triassic). During the second half of the Triassic, the Orot volcanic system was crosscut by granitoid intrusions of the Late Kunalei and Sogota complexes, 224.8 ± 1.3 Ma (Gordienko, 1987; Lykhin and Yarmolyuk, 2015). The localization of the beryllium mineralization at the deposit resulted from interaction between the derivatives of the alkali granite magma and the volcanic host rocks (Lykhin and Yarmolyuk, 2015).

Studies of fluid inclusions in the minerals of granitoids led to the conclusion that the Ermakovskoe and Orotskoe deposits are related to an alkali (aegirine) granite massif of the Late Kunalei Complex. Furthermore, ore-bearing fluids were released first within the Ermakovskoe and then within the Orotskoe deposit. That is why the ore productivity of the Ermakovskoe intrusion was five times as high as that of the Orotskoe deposit (Reif, 2007). Seven orebodies with a thicknesses of 5–30 m, strike length of 60–90 m, and dip length of 70–160 m were recognized within a 350- to 400-m-wide belt, which has been confirmed northwestward (320°–330°) for a distance of up to 700 m, at the Orotskoe deposit. The orebodies are grouped in two zones with a total thickness of 45–65 m and strike and dip lengths of 150–180 m, located 65–75 m from each other and confirmed by drilling to a depth of 250 m. The BeO distribution in ores is extremely irregular; its content varies from 0.005 to 1–2%. The orebodies have no distinct contacts with host rocks; their outlines have been established from sampling data (Kupriyanova and Shpanov, 2011).

In general, the Orotskoe deposit is attributed to the bertrandite ore formation and the economic ore type of bertrandite–argillizite metasomatites. The igneous rocks and ores of the Orotskoe deposit are believed to

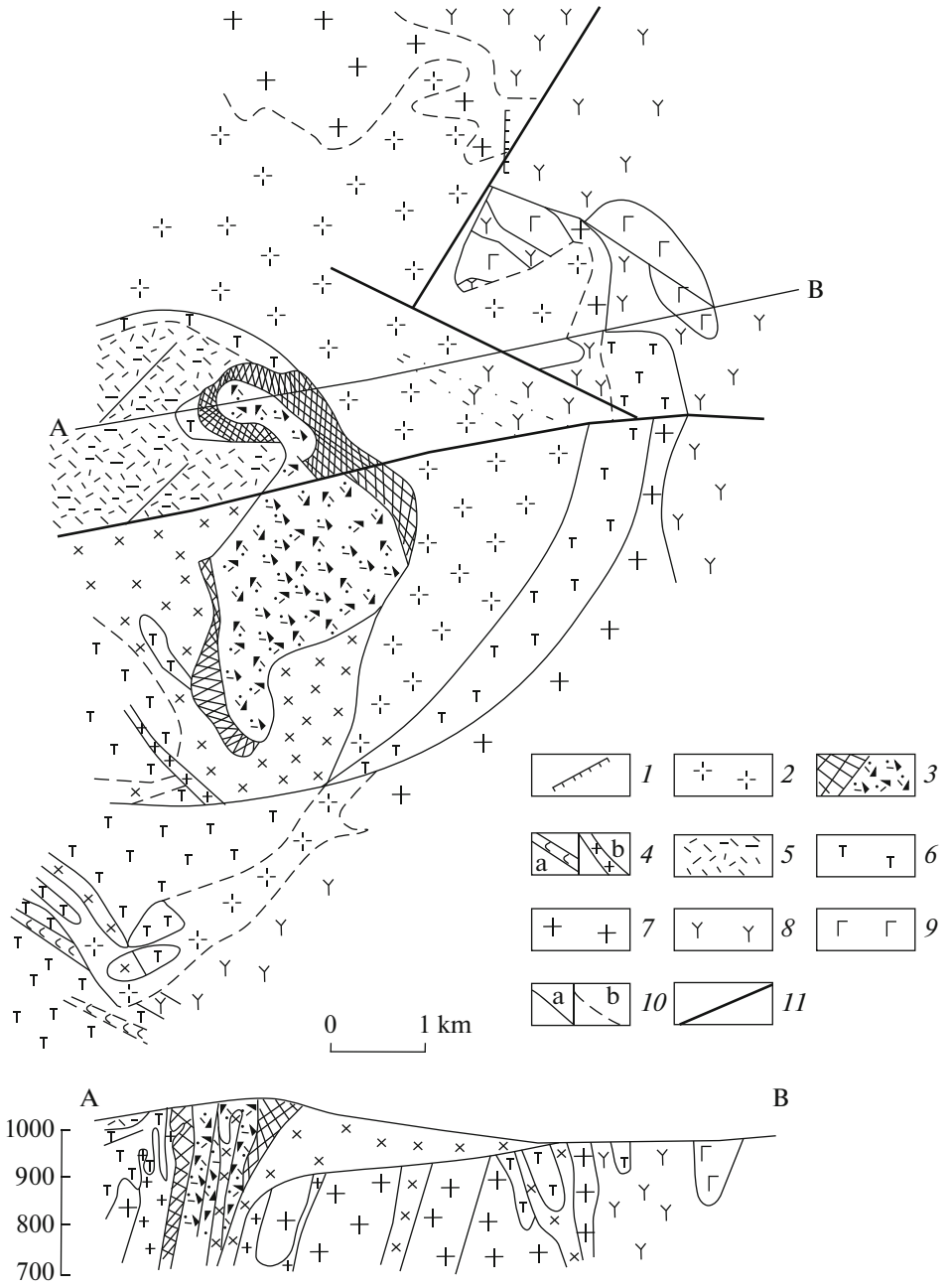


**Fig. 10.** Geological sketch map of Orot paleovolcano and associated bertrandite deposit. Compiled by I.V. Gordienko (1987) using materials of V.V. Skripkina and L.I. Reif (PGO Buryatgeologiya). (*1–4*) Sogota subvolcanic complex, Middle–Late Triassic: (*1*) syenite porphyry dikes; (*2*) laccolithic fine-grained porphyry granite body; (*3*) eruptive trachyrhyolite porphyry breccias of vent and near-vent facies; (*4*) dikes and stocks of porphyritic trachyrhyolites (a) and porphyry syenites (b); (*5*) Alentui Formation, Late Permian: trachyrhyolites with underlying rock fragments; (*6*) Suzha formation, Early Permian: trachybasalts, trachyrhyolites, trachytes, and basaltic andesites and respective tuffs and tuffstones with cordaite flora; (*7–9*) Kunalei and Bichura intrusive complexes, Late Permian: (*7*) medium-grained porphyritic granites, (*8*) medium- and coarse-grained syenites, (*9*) medium- and coarse-grained gabbro-syenites; (*10*) geological boundaries, proven (a) and inferred (b); (*11*) faults.

have formed with the participation of N-MORB and EM-II mantle sources with continental crustal contamination, which is evidenced by positive values of $\varepsilon_{Nd}(T) = +2.4$ (Lykhin et al., 2004).

In addition to the Kizhinga ore cluster with economic beryllium deposits, the Selenga ore district comprises the Tashir ore cluster including the Narynskoe and Taezhnoe fluorite deposits and the moderately sized Urminskoe beryllium deposit.

*The Urminskoe helvine–bertrandite deposit* was discovered in 1970 and studied in detail by geologists of the Buryatian Geological Survey and VIMS. It is

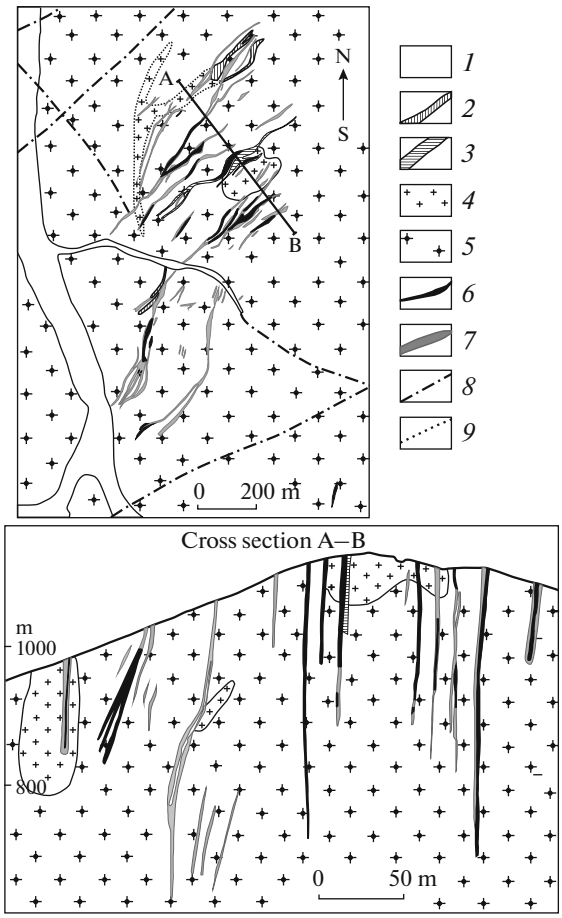


**Fig. 11.** Geological sketch map of Urminskoe helvine–bertrandite deposit and cross section A–B. After (Novikova and Zabolotnaya, 1988; Lykhin and Yarmolyuk, 2014). (*1*) Quaternary sediments; (*2–5*) Tashir intrusive complex, Early Mesozoic: (*2*) fine-grained syenite and porphyry syenite dikes; (*3*) andesite, trachyandesite, and diorite dikes; (*4*) fine-grained and inequigranular leucocratic granites, (*5*) medium-grained leucocratic granites; (*6*, *7*) quartz–feldspar metasomatites with helvine and bertrandite: (*6*) more than 0.1% BeO, (*7*) 0.06–0.1% BeO; (*8*) faults; (*9*) inferred fine-grained leucocratic granite boundaries.

located in the eastern part of the Lesser Khamar-Daban Range, at the junction of large faults, and comprises several ore occurrences: the Ubur–Tashirskoe, Levoberezhnoe, and Nizhnee Orelokskoe (Fig. 11). The deposit is confined to Early Mesozoic peralkaline granitoids of the Tashir intrusive complex, the equivalent of Late Kunalei granitoids (Kupriyanova et al., 2011; Lykhin and Yarmolyuk, 2014).

The beryllium mineralization is localized in the Ubur–Tashir massif, which is composed of leucogranites, alkali granites, and alkaline syenites (Kupriyanova and Shpanov, 2011). Dikes are scarce in this massif and consist of porphyry diorites and porphyry syenites. The ore mineralization is represented by helvine and bertrandite imprinted on the granite matrix. Ore zones of the deposit are zones of granite microclinization and albitization accompanied by beryllium mineralization and sulfidization (Novikova and Zabolotnaya, 1988). The ore zones at the deposit are controlled by steeply dipping oblique-slip faults and shear fractures. These faults and fractures provided pathways for hydrothermal solutions that induced metasomatism and ore localization. The ore zones contain en-echelon veiny, lenticular, and irregularly shaped orebodies that extend predominantly northeastward (10°–45°) and dip northwestward at 50°–70°. Twenty-three orebodies with a length of 50–200 m and an average thickness of 0.6–3.14 m have been identified. Some orebodies have been confirmed downward to a depth of more than 200 m. Bertrandite occurs predominantly at the upper levels, and helvine, at deeper ones (Lykhin and Yarmolyuk, 2015). The average beryllium oxide content in the orebodies varies from 0.131 to 0.852%. At the same time, zones fluorite-enriched are depleted in beryllium. Commercial evaluation of the deposit requires detailed exploration and further ore composition and age studies.

**Titanium.** The Arsent'evskoe titanium deposit and the Verkhne-Zuiskoe titanium occurrence are located west of the Kunalei ore cluster. They are associated with gabbros of the first phase of the Bichura Complex (Early–Late Permian). In terms of genesis, the titanium mineralization is classified as magmatic and attributed to the apatite–titanomagnetite gabbro–anorthosite ore formation.

*The Arsent'evskoe titanium deposit* is located in the Monostoi Range, in the central part of the gabbro–anorthosite massif of the same name (Fig. 12). The major ore minerals are magnetite and ilmenite; sulfides—pyrite, pyrrhotite, chalcopyrite, marcasite, and pentlandite—are present in small amounts. Apatite and green spinel are ubiquitous (Badmatsyrenova and Badmatsyrenov, 2011).

Based on mining working intercepts and magnetic data, 17 ore zones 11–300 m in thickness and 132–1040 m in length, located 30–190 m from each other, have been recognized. They have been confirmed downdip to a depth of 144–354 m. The strike of the zones is northeastward (50°–70°); the dip is southeastward at 20°–60°. They have been delineated based on a titanium dioxide cutoff grade of 4%. More than 90 lenticular, veined, or irregularly shaped orebodies measuring 3–10 × 50–60 m and possessing disseminated, thickly disseminated, and massive ores have been recognized in the zones. The percentages of ore minerals are 80–90% in massive ores, 40–60% in thickly disseminated ores, and up to 40% in disseminated ores. The ores contain 3–25% apatite, up to 15% green spinel, up to 7% pyrite, up to 2% chalcopyrite, and up to 16% pyrrhotite. The sulfide content slightly increases with depth. The proportions of magnetite and ilmenite in ores are usually equal, but magnetite prevails (sometimes two- to threefold) in massive and,

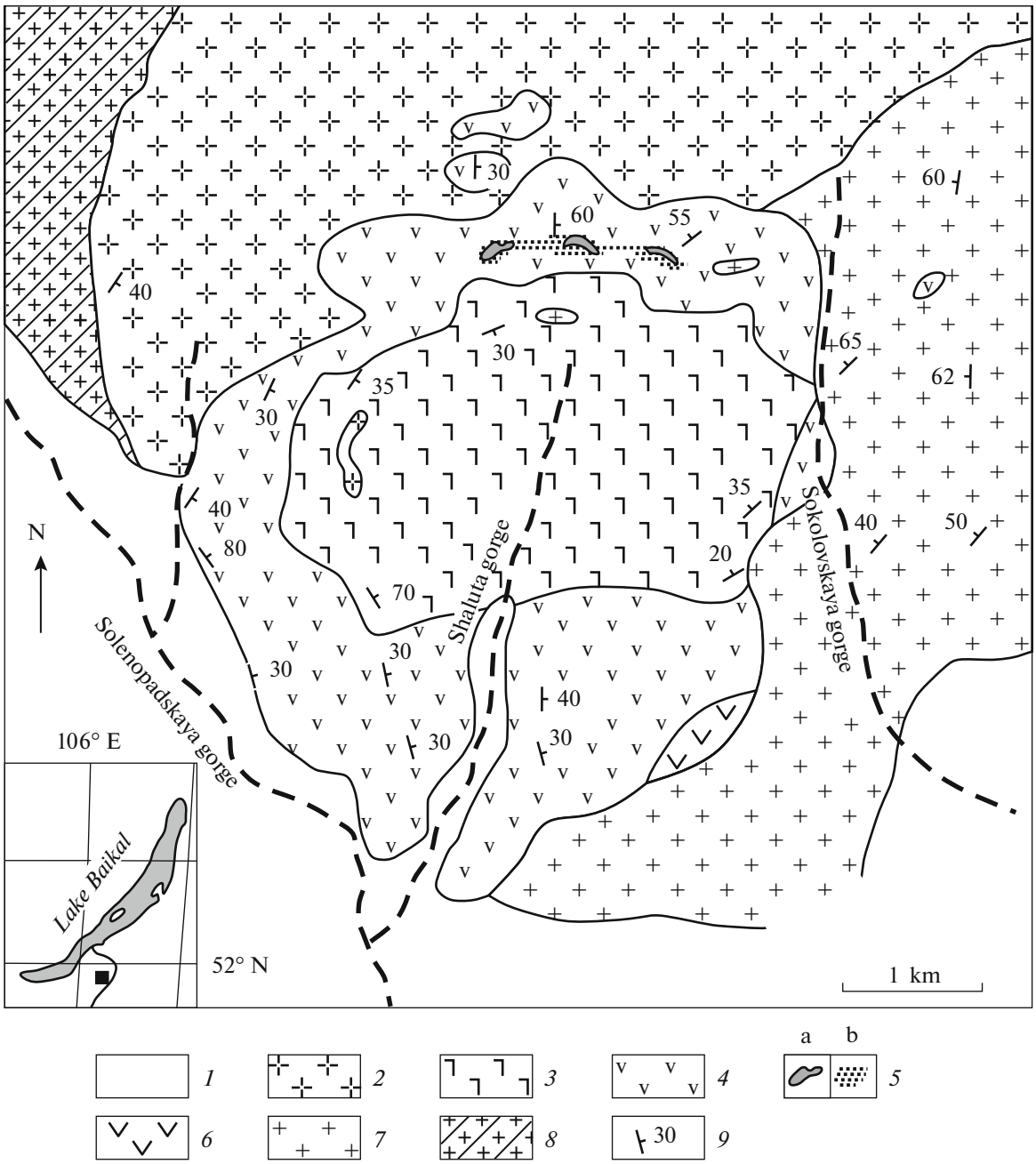


**Fig. 12.** Geological sketch map of Arsent'evskii gabbro–anorthosite massif. After (Badmatsyrenova and Badmatsyrenov, 2011).(*1*) Quaternary sediments; (*2*) syenites; (*3*) anorthosites and leucogabbros; (*4*) trachytoid olivine gabbros, monzodiorites; (*5*) ilmenite–titanomagnetite ores, massive (a) and disseminated (b); (*6*) gabbros, kaersutite gabbros, and pyroxenites; (*7*) diorites, granodiorites, and monzonites; (*8*) granite-gneisses; (*9*) strike and dip of trachytoid fabric.

partially, in rich disseminated ores. Disseminated ores are the most widespread. The average grades vary: 4.09–6.37% $TiO_2$, 14.68–27.96% total iron oxides, 1.61–3.1% $P_2O_5$, and 0.02–0.075% $V_2O_5$. The deposit is considered large. $TiO_2$ reserves with a cutoff grade of 4% are 299207 kt (Gusel'nikov, 1959unp; Smirnov et al., 1958unp). The U–Pb (SHRIMP II) zircon age of gabbros at the Arsent'evskoe deposit was determined at 279 ± 2 Ma (Badmatsyrenova et al., 2011).

The Verkhne-Zuiskoe occurrence is confined to a gabbro massif of the same name, located in the axial part of the Monostoi Range. The massif is composed of leucogabbros and olivine gabbros and less frequent gabbro–anorthosites and anorthosites. The average $TiO_2$ grade for the massif is 2.84%. The most ore-rich are leucogabbros containing 3 to 7.74% $TiO_2$. The olivine gabbros and gabbro–anorthosites are characterized by much lower $TiO_2$ grades, 1.71 and 1.95%,

respectively. The ore mineralization is unevenly distributed and represented by ilmenite and titanomagnetite. Three types of mineralization have been recognized: lean disseminated, disseminated, and occasional rich disseminated. $TiO_2$ grades are 3–5% in the lean disseminated ores, and 5–7% in disseminated ores. Three ore zones with lateral dimensions of 2250 × 254, 2270 × 261, and 1120 × 229 m have been recognized. Total category $C_2$ $TiO_2$ reserves of these zones are estimated at 317.3 Mt (Gusel'nikov, 1959unp).

**Gold.** Rich gold occurrences are unknown in the Selenga ore district. Occasional primary gold occurrences are represented by gold–quartz and gold–silver–sulfide ore formations and are attributed to the hydrothermal–postmagmatic plutonogenic type (Tret'yakovskoe deposit and Altacheiskoe, Virkhe, Vershinnoe, Oseredysh, and Izgib occurrences). The deposit and occurrences have not been mined, according to official data.

*The Tret'yakovskoe polymetal gold–fluorite–silver ore deposit* consists of gold-bearing quartz–fluorite veins, silicification zones, and stockworks (Fig. 13). The deposit is attributed to the quartz–fluorite–gold ore formation type.

Ore mineralization is located in northeast trending, steeply dipping crush zones confined to the feather joints of the Arshan Fault in the Khalyuta River basin. Five closely spaced quartz–fluorite veins with a length of 100–1150 m and a thickness of 0.05 to 3.1 m have been mapped in a zone measuring 4 × 1.5 km. Five 150- to 200-m-long and 0.2- to 3.0-m-thick silicification zones with gold–silver mineralization were recognized. The gold-bearing zones were explored on the surface and, in places, downward by borehole core sampling. The gold grade in these zones varies from 0.3 to 19.4 g/t, averaging 3 g/t; silver grades, from 1.9 to 18.6 g/t, averaging 7 g/t. Mineralization displays vertical zoning. Sulfides at deep levels of the quartz–fluorite vein no. 2 occur as rich impregnations up to 20 vol % in quartz and are represented by pyrite, pyrrhotite, chalcopyrite, and stannite. An increase in gold grade and orebody thickness with depth has been observed in some wells. The only potentially mineable orebody is vein no. 2, which was confirmed over a distance of 1150 m along strike with an average thickness of 1.04 m. The category $P_2$ resources of vein no. 2 were estimated at 3.3 t gold and 7.7 t silver. In the case of integrated development, the occurrence may prove economically viable.

The Altacheiskoe occurrence is confined to the North Zagan Fault. Stockwork-type silicification zones with copper–molybdenum (malachite–chalcopyrite–molybdenite) and gold mineralization were penetrated by drilling (Ochirov et al., 1992unp). Based on the results of channel sampling in trenches, the rocks contain 0.06–1% copper, 0.0008–0.02% molybdenum, 0.1–30 g/t silver, and 0.002–0.02 g/t gold. Core samples returned 0.01–0.3% copper and 0.0003–0.01% molybdenum. Malachite, chalcopyrite, limonite, magnetite, hematite, scheelite, fahlore, and apatite were identified in crushed samples; molybdenite, pyrite, arsenopyrite, fluorite, and azurite were encountered as single fine particles. This polymetal copper–molybdenum and gold–silver occurrence requires further exploration.

The Virkhe area in the Novopavlovka ore cluster is characterized by a weighted average gold grade of 0.1405 g/t. Argillization, silicification, pyritization, and fluoritization zones with a thickness of 50–100 m have been recognized here in the foliated felsic–intermediate volcanic rocks of the Alentui Formation ($P_2$). Based on channel sampling data, the gold grade in these zones does not exceed 1–1.5 g/t (usually several tenths or hundredths of g/t); only one sample returned 50 g/t gold. Category $P_2$ gold resources are estimated at 10150 kg (Koshkin et al., 2002unp).

**Uranium.** Uranium mineralization in the Selenga ore district is represented by two deposits and nine occurrences (Voronov, 1999unp). Two genetic types have been recognized: hydrothermal postmagmatic plutonogenic and hydrogenic. The hydrothermal uranium mineralization occurs in the Mesozoic volcano–tectonic depressions; it is represented by the Zhuravlinoe and Slantsevoe deposits and the Khangaiskoe, Verkhne-Ubukunskoe, and Vasil'evskoe occurrences. This mineralization is classified as the uranium ore formation in argillizites and feldspathic metasomatites of volcanotectonic structures and is usually associated with crush zones. Secondary alterations were reported in the form of silicification, feldspathization, argillization, fluoritization, pyritization, and chloritization. Uranium deposits and occurrences are characterized by similarity in geological structure (Zaitsev, 2013).

**Fluorite.** Almost 150 fluorite deposits and occurrences have been discovered in Western Transbaikalia. One moderately sized and 11 small fluorite deposits and 16 fluorite occurrences have been discovered in the Selenga ore district. The deposits and occurrences are attributed to the hydrothermal postmagmatic genetic type and the fluorite–quartz argillizite ore formation; they are characterized by a similar geological structure, ore quality, and technological characteristics (Bulnaev, 1995). Most fluorite deposits and occurrences of the Selenga ore district are located in the Tashir (Naranskoe deposit) and Novopavlovka (Nizhne-Chikoiskoe deposit) ore clusters.

*The Naranskoe deposit* is classified as epithermal and located in the southwestern endomorphic contact zone of the Ubur–Tashir granitoid massif (Fig. 14). Seventeen orebodies have been discovered and explored at the deposit. The orebodies of the deposit are represented by dilation veins and mineralized crush zones controlled exclusively by normal and oblique-slip faults. The ore controlling faults are, as a rule, high dipping with frequent changes in strike and dip directions. Some faults are strongly kinked along

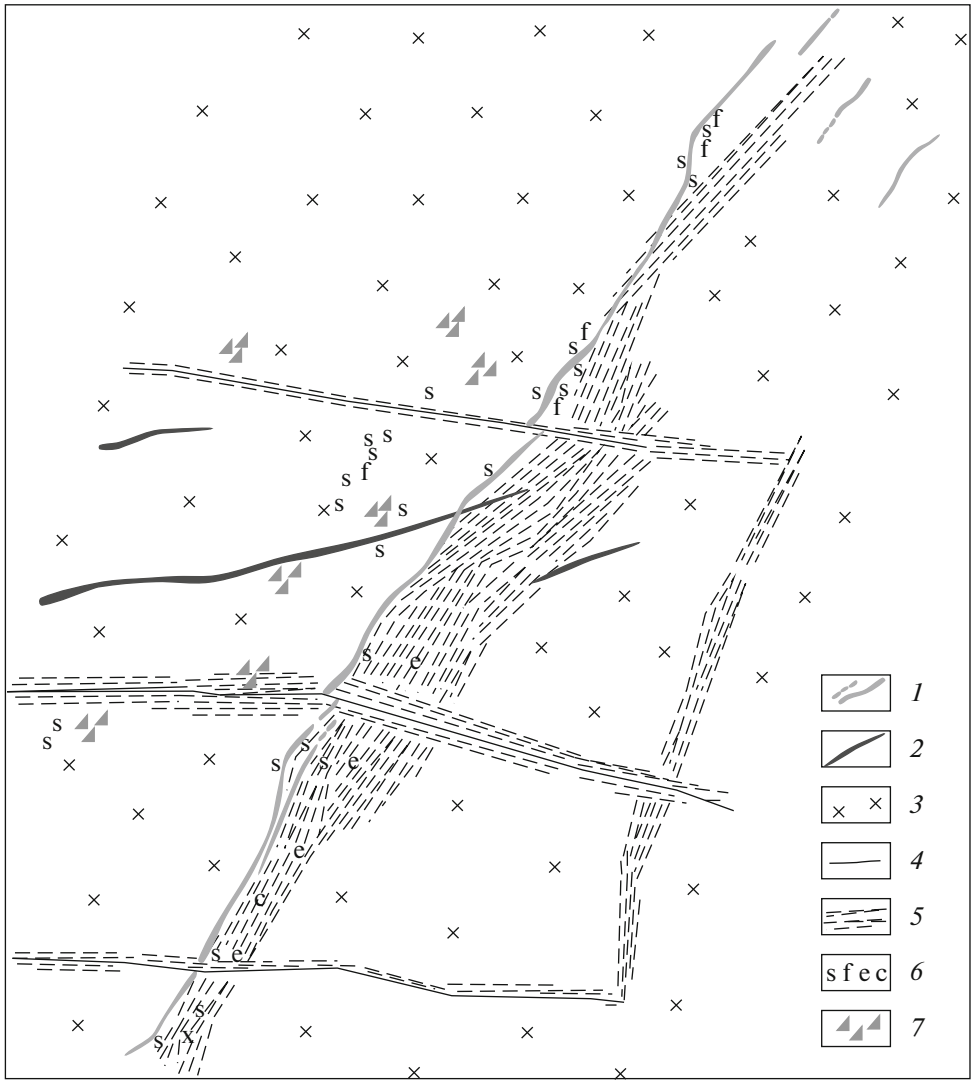


**Fig. 13.** Geological sketch map of Tret'yakovskoe polymetal ore deposit at 1 : 10 000 scale. After (Ivchenko, 1968unp). (*1*) Quartz–fluorite veins with gold; (*2, 3*) Bichura intrusive complex ($P_{1-2}$): (*2*) porphyritic diabase dikes, (*3*) biotite syenites; (*4*) faults; (*5*) extensive crush, brecciation, and mylonitization zones; (*6*) silicification, fluoritization, epidotization, and chloritization; (*7*) floats of quartz–fluorite ore fragments with gold.

strike and supplemented by complex splay fault systems. In addition, N–S trending faults crosscut and offset NE trending normal and strike-slip faults. The largest swells of frequently lenticular quartz–fluorite veins and mineralized zones are confined to these structurally complex segments of the N–S trending faults (Bulnaev, 1995). The mineral composition of the ores of the Naranskoe deposit depends on the types of orebodies they make up. Dilation veins are composed almost entirely of fluorite and quartz in various proportions. For mineralized crush zones, these two major vein minerals are supplemented by minerals of the host granosyenites: feldspars, quartz, biotite, and hornblende. The most frequently encountered minor minerals, related to hydrothermal fluorite formation, are clay minerals such as kaolinite, montmorillonite, and illite. They concentrate in mineralized crush zones and wallrock argillization zones. Rock structures at the deposit are diverse, but three types are predominant in economic orebodies: brecciated, massive, and vein–disseminated.

Ores of the Naranskoe deposit contain 25.5–34.32% fluorite, 34.73–55.17% quartz, and 16.55–62.9% feldspar on average. The amounts of carbonates, sulfur, phosphorus, and iron, which are considered harmful impurities in fluorite ores, are insignificant and usually do not exceed a few hundredths or thousandths of a percent (Bulnaev, 1995). Total category $A+B+C_1$- explored reserves of fluorite ores are 1621 kt with average grade of 31.15% (Table 1).

**Rare-earth elements.** A large rare-earth carbonatite province has been recognized in Western Transbaika-

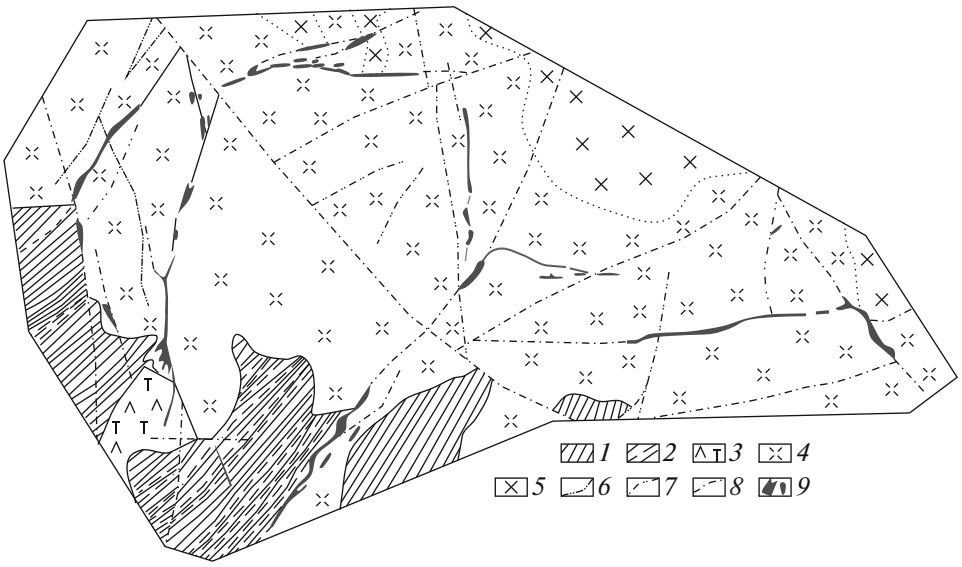


**Fig. 14.** Geological sketch map of Naranskoe fluorite deposit at 1 : 2000 scale. After (Bulnaev, 1995). (*1–2*) Neoproterozoic (Astai Formation): (*1*) biotite–quartz–feldspar schists, (*2*) amphibole–biotite schists; (*3–7*) Tashir intrusive complex, Late Permian–Early Triassic: (*3*) trachyandesites, (*4*) porphyry syenites and syenites, (*5*) granosyenites, (*6*) micropoikilitic and felsitic porphyry dikes, (*7*) diorite, andesite, and trachyandesite porphyry dikes; (*8*) faults; (*9*) fluorite and quartz–fluorite bodies.

lia (Ripp et al., 2000; Nikiforov et al., 2000, 2002). Complex rare earth–barium–strontium mineralization associated with the Early Cretaceous carbonatites of the Khalyuta Complex has been discovered within it (Ripp et al., 2009). The Khalyutinskoe, Verkhne-Khalyutinskoe, Arshan–Khalyutinskoe, and Verkhne-Shalutaiskoe REE occurrences were discovered in the Cheremshana–Oshurkovo ore cluster, on the northern flank of the Ivolga Depression, along the Gil'bira Fault (Radchenko et al.,. 1978unp; Goldberg, 1990unp). In addition, carbonatites were discovered within the Oshurkovo apatite-bearing massif (Nikiforov et al., 2000, 2002; Ripp et al., 2013).

*The Khalyutinskoe strontium, barium, and REE occurrence* was covered by prospecting and appraisal surveys. It is confined to a dikelike carbonatite body ~100 m in thickness that dips westward at 30°–40° (Fig. 15). The carbonatites were confirmed by drilling to a depth of 187 m; their intrusive contacts with Neoproterozoic metamorphic host rocks were established. The carbonatites are barium–strontium ores with average grades of 10.17% SrO, 8.42% BaO, and 0.21% REE. The ores are characterized by banded, lenticular–banded, and brecciated structure and consist of calcite, barite–celestite, strontianite, magnetite, apatite, and phlogopite. Bench testing at the State Scientific Research Institute of Chemical Feedstock Mining (GIGKS) confirmed the theoretical possibility of extracting strontium hydroxide directly from the ore without acids or costly deficient chemical agents. Lime as a by-product can be used in civil construction. Undiscovered category $P_1 + P_2 + P_3$ strontium oxide resources are estimated at 11100 kt (see Table 1). This occurrence is assumed to be promising and is recommended for first-priority development.

The U-Pb (SHRIMP II) zircon age of the carbonatites of the Khalyutinskoe occurrence, determined on a zircon from the main orebody (Ripp et al., 2009), is 130 ± 1 Ma. Previous researchers (Bulnaev and Posokhov, 1995) determined the Rb–Sr age at 119 ± 10 Ma.

Ores at the Arshano–Khalyutinskoe carbonatite occurrence are characterized by brecciated–banded structures and consist of calcite, phlogopite, biotite, bastnaesite, barite–celestite, strontianite, monazite, fluorite, magnetite, and hematite. The content of total cerium-group (predominant) and yttrium-group REE oxides in carbonatites varies from 0.87 to 7.64%; barium and strontium, up to 3%; fluorite, 11%. $P_2$-category total REE resources are estimated at 186 kt; fluorite, 434 kt. The Arshano–Khalyutinskoe and other carbonatite occurrences (see Fig. 15) require further exploration.

**Apatite.** The apatite-bearing magmatic rocks occupy a significant position in the Selenga ore district. The Oshurkovskoe apatite (phosphorus ore) deposit and a number of promising ore occurrences are located here (Andreev et al., 1972).

*The Oshurkovskoe deposit*, which is located on the outskirts of Ulan-Ude, is the largest apatite deposit in the region. It was explored by geologists of the Buryatian Geological Administration and was considered to be associated with a Late Proterozoic diorite and syenodiorite massif (Kostromin et al., 1969unp). Later, the predominantly plutonogenic–postmagmatic genetic type related to the emplacement of the Paleozoic apatite-bearing subalkaline gabbrodiorites

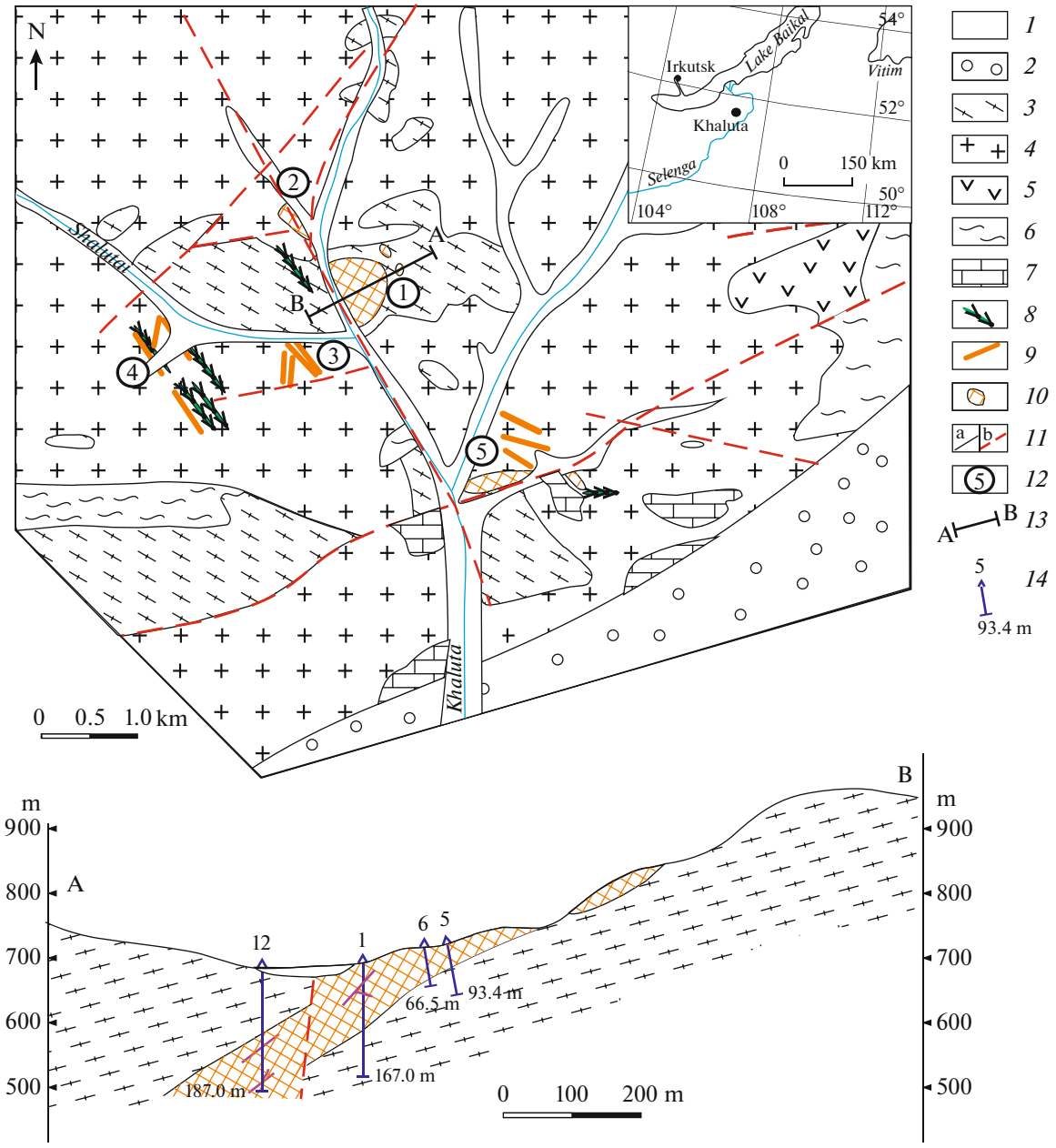


**Fig. 15.** Geological sketch map of Khalyutinskoe deposit and other carbonatite occurrences. Exploratory cross section A–B of Khalyutinskoe carbonatite body. After Radchenko et al. (1978unp). (*1*) Quaternary sediments; (*2*) conglomerates and sandstones; (*3*) gneissose granites; (*4*) quartz syenites; (*5*) gabbro; (*6*) schists; (*7*) marbles; (*8*) shonkinite and alkaline syenite dikes; (*9*) carbonatite dikes; (*10*) blanketlike carbonatite bodies; (*11*) faults: (*a*) proven, (*b*) inferred; (*12*) carbonatite occurrence areas: Khalyutinskii (1), Verkhne-Khalyutinskii (2), Nizhne-Shalutaiskii (3), Verkhne-Shalutaiskii (5), Arshan–Khalyutinskii (4); (*13*) section line; (*14*) boreholes in cross section.

and syenodiorites, which are widespread in Western Transbaikalia, was confirmed in number of studies based on exploration data and the results of detailed structural–geological and petrographic studies (Gordienko, 1970; Andreev et al., 1972). It was established that the Oshurkovskoe deposit should be attributed to the apatite–diorite–gabbroid ore formation and the geological–industrial type of apatites in apogabbro syenodiorites. The deposit was covered by detailed exploration and prepared for mining (Savel'ev et al., 1988unp). It is confined to a massif of subalkaline gabbroids that covers 12 km$^2$ and has a close to isometric shape in plan view. The orebody occupies the majority of the massif. Apatite is among the main rock-forming minerals in the Oshurkovskoe deposit; its content varies from 3–4 to 15–20%. Elevated apatite concentrations are found in melanocratic fine- and medium-grade rock varieties. Several areas with a width of 100–

400 m, length of 500–600 m, and $P_2O_5$ content of 5–6% have been recognized in the massif. They make up a 500- to 600-m-wide belt extending 2.0–2.5 km across the central part of the massif. Total category $A + B + C_1$ reserves to a depth of 200 m are estimated at 108.6 Mt $P_2O_5$ with an average grade of 3.8%, cutoff grade of 2.5%, and minimum economic grade of 3.6%. Undiscovered category $P_1$ resources to a depth of 500 m are estimated at 137 Mt $P_2O_5$ (Table 1).

Recently, mineralogical–geochemical and isotopic–geochronological studies were carried out at the Oshurkovskoe massif and the apatite deposit of the same name. The results demonstrate that, in addition to the economic apatite mineralization associated with the subalkaline gabbroid intrusion, carbonatite veins with apatite mineralization formed later (during the Cretaceous) (Nikiforov et al., 2000, 2002; Tsarev and Batueva, 2013; Ripp et al., 2013).

**Quartz.** The Cheremshanskoe premium quartzite deposit is a large source of strategic raw material in the Selenga ore district.

*The Cheremshanskoe deposit* is located 60 km from Ulan-Ude and 40 km from the Tataurovo Station of the East Siberian Railway. It was discovered in 1965–1966 among Neoproterozoic clastics of the Itantsa Formation in Eastern Cisbaikalia by the Zyryanskaya Party of the Buryatian Geological Administration as a result of 1 : 50000 geological mapping (Sokolov and Plotnikov, 1972unp). It was later established that this silicon deposit is a large source of high-purity quartzitic sandstones (Borisov et al., 1999; Tsarev et al., 2007) (Fig. 16).

The deposit consists of large (more than 10 km) white monomineral quartzite and quartzitic sandstone ledges 30 to 50 m in thickness. White and yellowish-white quartzitic sandstones consist of quartz grains (99.2% silica) free of gas-fluid and mineral inclusions. Detrimental impurities (0.7–1.0%) are iron oxides, which are easily removed. Quartzite reserve estimates as of January 1, 2007, are as follows (kt): B-category, 2397; category $C_1$, 10443; category $C_2$, 2275; of that, 2521 kt of category B and 8156 kt of category $C_1$ reserves are located within the limits of the open pit. The impurity contents are as follows: 0.1% $Fe_2O$, 0.2% $Al_2O_3$, and 0.005% CaO. In terms of composition, mineralogical and structural features, and physical parameters the quartzitic sandstones have a virtually uniform technological type that complies with industrial requirements for industrial silicon, silicon carbide, and ferrosilicium production.

There are other large premium quartz deposits in the Republic of Buryatia (Chulbonskoe, Atarkhanskoe, Bural–Sardykskoe, etc.), and the republic possesses all prerequisites for becoming a major producer and exporter of polycrystalline silicon and autonomous energy supply systems of up to one-third the total global turnover (Bakhtin et al., 2007; Yalovik, 2010).

## GEODYNAMIC SETTINGS AND FORMATION CONDITIONS OF ORE DEPOSITS

The Late Paleozoic–Early Mesozoic (Middle and Late Carboniferous, Permian, and Triassic) geodynamic evolution of Transbaikalia, including the Selenga ore district, was guided by interaction between the Siberian continent and the Mongolia–Okhotsk Ocean (Zonenshain et al., 1990; Kovalenko and Yarmolyuk, 1990). This ocean, according to reconstructions, was a gulf of the Paleopacific Ocean during the latest Carboniferous and Permian (Golonka et al., 2006). The eastern margin of the Siberian continent was an Andean-type active continental margin at the time (Gordienko and Kuzmin, 1999; Donskaya et al., 2013).

It was established that volcanic eruptions began during the Middle–Late Carboniferous simultaneously with the inception of a large rift-related transregional structure, the Selenga–Vitim volcanoplutonic belt, at the rear of the active Siberian continental margin. The intense intraplate magmatism within the active continental margin led not only to the formation of Devonian–Early Carboniferous volcanotectonic structures of Western Transbaikalia in its rear part (Gordienko et al., 2010; Minina et al., 2016), but also to the widespread emplacement of granitoids of the Barguzin complex with radiometric ages of 330–290 Ma, which formed the world's largest Angara–Vitim batholith, covering ~150000 $km^2$ (Kuzmin and Yarmolyuk, 2014; Tsygankov et al., 2017). The participation of mantle sources in batholith formation facilitated heating of the territory of Western Transbaikalia, which later led to crust–mantle interaction and the subsequent formation of closely interrelated volcanic sequences, basites, and granitoids with varying alkalinity and acidity.

The initial trachyandesite–rhyolite eruption events (Gunzan Sequence) took place on the northern and southern flanks of the belt and at its western terminus. This igneous event continued during the Middle–Upper Carboniferous and Early Permian. The following plutonic rock associations have been recognized (from earliest to latest): (1) calc-alkaline and subalkaline granites and quartz syenites with synplutonic basites of the Zaza Complex, dated at 305–285 Ma; (2) quartz syenites and monzonites with basites of the Lower Selenga Complex dated at 285–278 Ma. The composition of plutonic rocks of the Zaza and Lower Selenga complexes supports their crustal–mantle origin (Gordienko and Tsygankov, 2017). These magmatic processes are manifested at a large distance from the Angara–Vitim batholith, in southwestern Transbaikalia and northern Mongolia.

Later, the geodynamic setting was complicated by the development of rift-related volcanotectonic structures in the rear of the active continental margin during the Late Permian and Early Triassic. The Late Permian was marked by areal trachybasalt eruptions

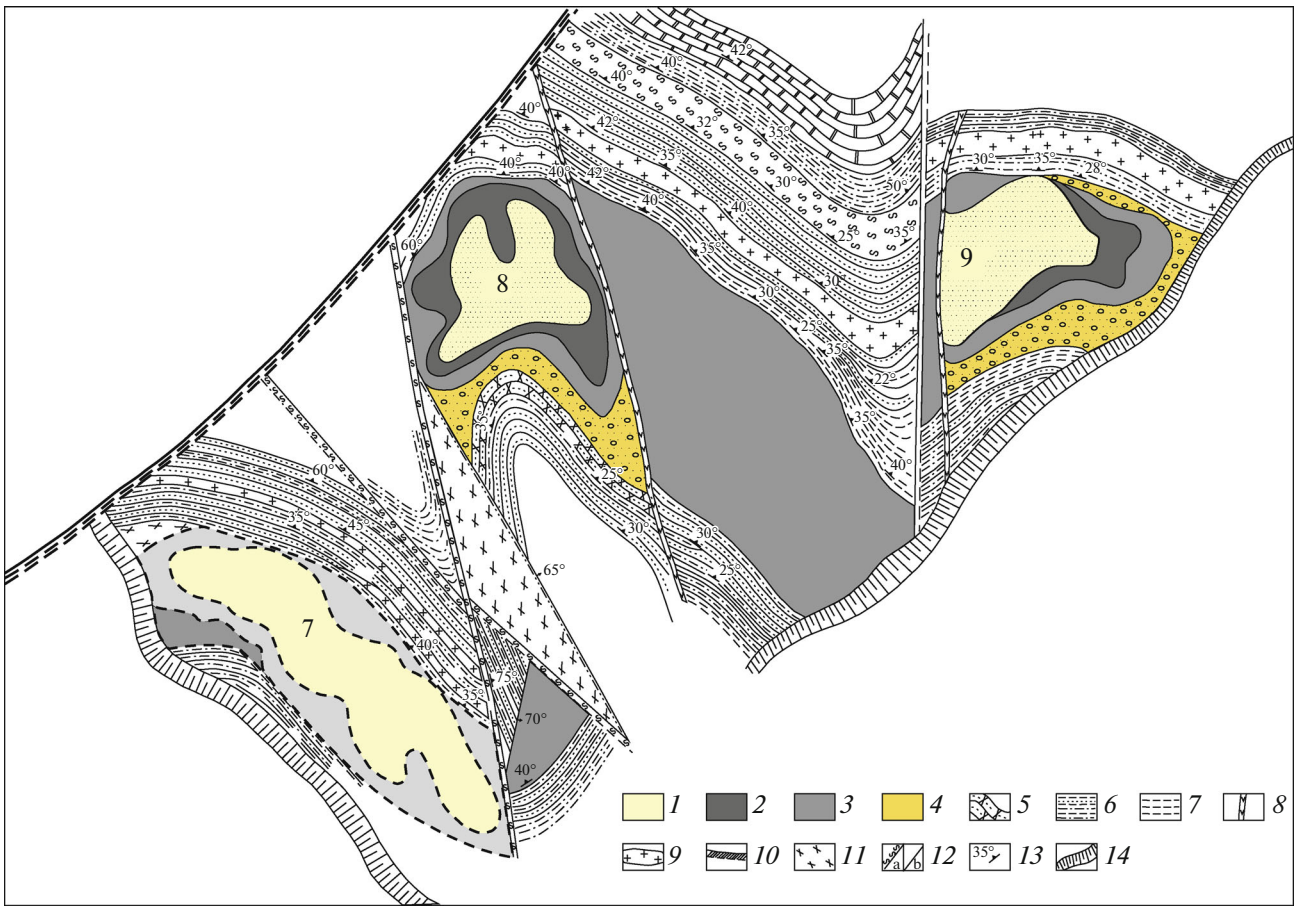


**Fig. 16.** Geological sketch map of quartz ledges nos. 7, 8, and 9 of Cheremshanskoe quartz deposit at 1 : 1000 scale. After Gal'chenko (1999unp). (*1*) White high-purity quartzites; (*2*) yellowish–white quartzites; (*3*) yellowish–gray quartzites with occasional shadows of replaced sandstones; (*4*) yellow sandstones with frequent relics of replaced sandstones; (*5*) quartz sandstones with carbonate cement; (*6*) sericite bearing quartzites alternating with quartz–sericite schists; (*7*) carbonaceous quartz–sericite schists and phyllites; (*8*) porphyritic diorite dikes; (*9*) kaolinized aplitic granite sills; (*10*) clay–iron oxide mineral pigments and carbonate–iron oxide aggregates; (*11*) variegated clays including clasts of crystalline rocks; (*12*) faults with wallrock mylonitization (a) and other faults (b); (*13*) strike and dip symbols; (*14*) working benches of opencast mine.

(the Ungurkui, Munustai, and Tamir sequences), which were accompanied by emplacement of dolerite and gabbro–syenite sills and laccoliths, as well as bimodal series with comendites and alkali granites of the Kunalei Complex. The latter are particularly widespread in the Selenga ore district and have been dated as Late Permian and Early Triassic.

The subsequent Early Mesozoic history of the geodynamic evolution of the region was also guided by the interaction between the Siberian continent and the Paleopacific Ocean including its gulf, the Mongolia–Okhotsk Ocean Basin. A complicated California-type or Mongolia–Okhotsk-type geodynamic setting existed during the Early Mesozoic along the present-day fold belts encircling the southern margin of the Siberian Craton in Transbaikalia, where the Mongolia–Okhotsk belt is currently located (Kovalenko and Yarmolyuk, 1990; Gordienko and Kuzmin, 1999). It was characterized by thrusting of the Siberian continent onto structures of the Mongolia–Okhotsk Ocean Basin, which led to the inception of "scattered" rifting and "disperse" magmatism. A distinguishing feature of this process was the combination of compression and extension settings, which accounts for the formation of numerous volcanotectonic structures consisting of intraplate volcanic rocks with rare metalliferous and other granitoids with various alkalinity and acidity in this region. The granitoids are associated with the main endogenic ore deposits of the Selenga ore district, which determine its metallogenic specialization.

Geochronological studies performed in recent years have made it possible to reconstruct the history of volcanic processes in the mentioned structures and to reveal their geodynamic setting. It was established that Mesozoic volcanic activity in Transbaikalia was concentrated in a number of volcanic regions and zones and controlled by mantle plumes of the mantle hot field (Yarmolyuk et al., 2017). Probably, the plume development dynamics was intermittent and impulsive. Each event of plume activity is represented by

a certain complex of volcanic and plutonic rocks associated with mineral deposits discovered in the Selenga ore district (Kovalenko et al., 2003; Gordienko and Tsygankov, 2017). It should be noted that similar processes in which the continuity of the lithosphere was breached by mantle plumes and the activity of ore-bearing fluid–magmatic flows was boosted for a long time presumably took place during localization of the orebodies in the Strel'tsovskoe molybdenum–uranium ore field in Eastern Transbaikalia and the Dzhida ore district (Petrov et al., 2017; Gordienko et al., 2018b).

Starting from the latest Triassic, extensive magmatic processes in the region continued virtually without interruption and led to the development of the Late Mesozoic–Cenozoic volcanic region (Yarmolyuk et al., 1998). The known rare-earth mineralization in the Selenga ore district, associated mostly with carbonatite formation, was localized during this stage.

## FORECASTS AND OUTLOOK FOR THE INDUSTRIAL DEVELOPMENT OF THE SELENGA ORE DISTRICT

It is known that the strategy of economic development of the Republic of Buryatia is based largely on the development of the resource base of noble, ferrous, alloying, nonferrous, and rare metals (molybdenum and tungsten) and fossil fuel resources. This includes strategically important metals—beryllium, gold, platinum, lead, silver, copper, nickel, chrome, titanium, and rare and rare-earth elements (Ignatovich, 2007; Ignatovich and Fil'ko, 1978; Bakhtin and Yalovik, 2007; Yalovik, 2010).

The Kurbi–Eravna, North Baikal, East Sayan (Oka), and Dzhida ore districts, which we studied earlier within a program of the RAS Presidium (Gordienko and Nefed'ev, 2015; Gordienko et al., 2014; 2016; 2018b), are presently considered large mining industry clusters that can provide the basis for the formation of the East Buryatian, North Baikal, and Oka–Dzhida territorial industrial complexes as centers of economic development of Siberia and the Republic of Buryatia in the future (*Mineral'no–syr'evoi* ..., 2009).

In this context, the easily accessible mineral resources of the Selenga ore district with economically well developed infrastructure are highly prospective and economically valuable (Bakhtin et al., 2007; Takhanova, 2017, Gordienko et al., 2018a). The large Ermakovskoe beryllium, Zharchikhinskoe molybdenum, Arsent'evskoe titanium, Oshurkovskoe apatite, and Cheremshanskoe quartzite deposits; the Khalyutinskoe rare metal–rare earth ore occurrence in carbonatites; and smaller underexplored molybdenum, beryllium, uranium, copper, gold, and other metals and minerals have been discovered and explored here. In the case of positive changes in the world market, all of them could be successfully used for economic modernization of the region and Russia as a whole.

## CONCLUSIONS

The bulk of economic strategic mineral resources of the Selenga ore district are related to Late Paleozoic–Early Mesozoic igneous activity. The active intraplate (rift-related) processes that took place during the Late Paleozoic–Mesozoic led to the formation of endogenic rare metal, titanium, gold, and REE ore deposits, as well as postmagmatic and hydrothermal–metasomatic apatite and quartz deposits. It has been established that the main role in these processes was played by mantle plumes and abyssal transmagmatic solution (fluid) flows, which concentrated at the upper levels of ore–magmatic systems, in fault and dike development zones. The plumes probably continued for a long time, from the Late Paleozoic to the Mesozoic inclusive, and their action was impulsive. This accounts for the different ages of magmatism and ore-forming processes in virtually all ore occurrences of the Selenga ore district.

New factual data on the minerogeny of the Selenga ore district provide the scientific basis for replenishing the mineral resource base of the Sayan–Baikal region and can be efficiently used during the construction of state-of-the-art integrated mining and processing plants and prospecting and evaluation of known and new ore occurrences.

## ACKNOWLEDGMENTS

We are grateful to Academician V.V. Yarmolyuk for critical remarks and comments, which helped to improve this article, and to M.Sh. Bardina and A.A. Kalenykh for technical assistance.

## FUNDING

This study was supported by the RAS Presidium (Program no. 1.4P "Deposits of Strategic Minerals in Russia: Innovative Approaches to Their Forecasting, Evaluation, and Mining") and partially by the Russian Foundation for Basic Research (project nos. 15-05-01633a and 18-45-030016 r_a).

## CONFLICT OF INTEREST

The authors declare that they have no conflict of interest.

## REFERENCES

Andreev, G.V., Gordienko, I.V., Kuznetsov, A.N., and Kravchenko, A.I., *Apatitonosnye diority Yugo-Zapadnogo Zabaikal'ya* (Apatite-Bearing Diorites of Southwestern Transbaikalia), Ulan-Ude: Buryatskoe knizhnoe izd-vo, 1972.

Andryushchenko, S.V., Vorontsov, A.A., Yarmolyuk, V.V., and Sandimirov, I.V., Evolutiom of Jurassic–Cretaceous

magmatism in the Khambin volcanotectonic complex (western Transbaikalia), *Russ. Geol. Geophys.,* 2010, no. 7, pp. 734–749.

Badmatsyrenova, R.A. and Badmatsyrenov, M.V., The sources of basic magmatism in western Transbaikalia in the Late Paleozoic (from geochemical and isotope data), *Russ. Geol. Geophys.,* 2011, vol. 52, no. 6, pp. 631–640.

Badmatsyrenova, R.A., Larionov, A.N., and Badmatsyrenov, M.V., Titanium-bearing Arsent'ev massif (western Transbaikalia): new SIMS U-Pb geochronological data, *Izv. Sib. Otd. Sektsii nauk o Zemle RAEN,* 2011, no. 1 (38), pp. 132–138.

Bakhtin, V.I. and Yalovik, G.A., State and prospects of the evolution of mineral-raw base of Buryat Republic, up to 2020, *Razvedka Okhr. Nedr,* 2007, no. 12, pp, 6–15.

Bakhtin, V.I., Yalovik, G.A., Gusev, Yu.P., Ignatovich, V.I., and L'vov, V.A. Main mineral resources of the Buryat Republic, *Razvedka Okhr. Nedr,* 2007, no. 12, pp. 15-21.

Baturina, E.E. and Ripp, G.S., *Molibdenovye i vol'framovye mestorozhdeniya Zapadnogo Zabaikal'ya (osnovnye cherty metallogenii i geokhimii)* (Molybdenum and Tungsten Deposits of Western Transbaikalia (Main Metallogenic and Geochemical Features), Moscow: Nauka, 1984.

Borisov, A.P., Gal'chenko, V.I., Mironov, A.G., and Korsunov, V.M., Cheremshansk quartzite as the basis for complex development of ore reserves of Buryat Republic, *Gorn. Zh.,* 1999, no. 3, pp. 1–4.

Bulnaev, K.B., Origin of the fluorite–bertrandite–phenakite deposits, *Geol. Ore Deposits,* 1996, vol. 38, no. 2, pp. 128–136.

Bulnaev, K.B., Naran deposit, *Mestorozhdeniya Zabaikal'ya* (Deposits of Transbaikalia), Moscow: Geoinformmark, 1995, vol. 1, book 2, pp. 197–203.

Bulnaev, K.B. and Posokhov, V.F., Isotope-geochemical data on the nature and age of endogenous carbonate rocks of Transbaikalia, *Geokhimiya,* 1995, no. 2, pp.189–196.

Donskaya, T.V., Windley, B.F., Mazukabzov, A.M., Kroner, A., Sklyarov, E.V., Gladkochub, D.P., Ponomarchuk, V.A., Badarch, G., Reichow, M., and Hegner, E., Age and evolution of Late Mesozoic metamorphic core complexes in southern Siberia and northern Mongolia, *J. Geol. Soc.,* 2008, pp. 405–421.

Donskaya, T.V., Gladkochub, D.P., Mazukabzov, A.M., and Ivanov, A.V., Late Paleozoic-Mesozoic subduction-related magmatism at the southern margin of the Siberian continent and the 150 million-year history of the Mongol–Okhotsk ocean, *J. Asian Earth Sci.,* 2013, no. 62, pp. 79–97.

Efimov, I.I., Kudarin molybdenum–copper porphyry occurrences, *Globus (Geologiya i Biznes),* 2010, no. 5 (13), pp. 42–46.

*Geologicheskaya karta yuga Vostochnoi Sibiri i Severnoi chasti MNR. Masshtab 1 : 1500000* (Geological Map of the southern part of East Siberia and Northern Mongolia on a Scale 1 : 1500000), A.L. Yanshin, Eds., Leningrad: Izd-vo Kartfabriki VSEGEI, 1980.

Ginzburg, A.I., Zabolotnaya, N.P., Novikova, M.I., and Gal'chenko, V.I., Genetic features of fluorite–phenakite bertlandite mineralization, *Razvedka Okhr. Nedr,* 1969, no. 1, pp. 3–10.

Golonka, J., Krobicki, M., Pajak, J., Van Giang, N., and Zuchiewicz, W., *Global Plate Tectonics and Paleogeography of Southeast Asia,* Arkadia; Krakov: AGN Univ. Sci. and Technol., 2006.

Gordienko, I.V., Apatite-bearing diorites of the Oshursk type as a new genetic type of apatite deposits, *V chteniya pamyati akademika S.S. Smirnova* (5th Smirnov Reading), Chita: Zabaikal. filiala geograf. obshchestva SSSR, 1970, pp. 135–138.

Gordienko, I.V., Evolution of Paleozoic magmatism and endogenous mineralization of folded framing of the southern Siberian Platform and geodynamic settings of its formation, *Tikhookean. Geol.,* 1992, vol. 11, no. 4, pp. 101–109.

Gordienko, I.V., Metallogeny of different geological settings of the Mongol–Transbaikalian region, *Geol. Mineral-Syr'ev. Res. Sibiri,* 2014, no. 3. pt. 1, pp. 7–13.

Gordienko, I.V., *Paleozoiskii magmatizm i geodinamika Tsentral'no-Aziatskogo skladchatogo poyasa* (Paleozoic Magmatism and Geodynamics of the Central Asian Fold Belt), Moscow: Nauka, 1987.

Gordienko, I.V., Composition and age of the Tamir Formation of the volcanogenic rocks of Western Transbaikalia, *Izv. AN SSSR, Ser. Geol.,* 1980, no. 7, pp. 84–91.

Gordienko, I.V., *Middle and Upper Paleozoic non-geosynclinal magmatism of the Sayan–Baikal mountainous area, Tektonika Sibiri (Tectonics of Siberia)*, Moscow: Nauka, 1976, vol. 7, pp. 82–90.

Gordienko, I.V., Bulgatov, A.N., Nefed'ev, M.A., and Orsoev, D.A., Geological-geophysical, forecasting-metallogenic studies, and prospects of development of mineral resources of the Northern Baikla ore district, *Izv. Sibirsk. Otd., Sekts. Nauk Zemle, Ross. Akad. Estestven. Nauk, Geologiya, Poiski Razvedka Rudn. Mestorozhd.,* 2014, no. 2 (45), pp. 5–18.

Gordienko, I.V., Bulgatov, A.N., Ruzhentsev, S.V., Minina, O.R., Klimuk, V.S., Vetluzhskikh, L.I., Nekrasov, G.E., Lastochkin, N.I., Sitnikova, V.S., Metelkin, D.V., Gonegger, T.A., and Lepekhina, E.N., The Late Riphean–Paleozoic history of the Uda–Vitim island-arc system in the Transbaikalian sector of the Paleoasian ocean, *Russ. Geol. Geophys.,* 2010, vol. 51, no. 5, pp. 461–481.

Gordienko, I.V., Gorokhovsky, D.V., Smirnova, O.K., Lantseva, V.S., Badmatsyrenova, R.A., Orsoev, D.A., Dzhida ore district: geology, structural and metallogenic regionalization, genetic types of ore deposits, geodynamic conditions of their formation, forecast, and outlook for development, *Geology of Ore Deposits*., 2018, vol. 60, no. 1, pp. 1–32.
https://doi.org/10.1134/S1075701518010038

Gordienko, I.V. and Klimuk, B.C., Bimodal volcanism of the Tugnui rift basin, Transbaikalia, *Geol. Geofiz.,* 1995, vol. 36, no. 5, pp. 23–37.

Gordienko, I.V. and Kuz'min, M.I., Geodynamics and metallogeny of the Mongol–Transbaikalian region, *Geol. Geofiz.,* 1999, vol. 40, no. 11, pp. 1545–1562.

Gordienko, I.V., Lantseva, V.S., Badmatsyrenova, R.A., and Elbaev, A.L., Selenga ore district of the Buryat Republic: geological structure, metallogeny, geodynamics, and prospects of evolution, *Izv. Sibirsk. Otd., Sekts. Nauk Zemle, Ross. Akad. Estestven. Nauk. Geologiya, Razvedka Razrabotka Mestorozhd. Polezn. Iskop.,* 2018a, vol. 41, no. 1, pp. 9–37.

Gordienko, I.V. and Nefediev, M. A., The Kurba-Eravna ore district of Western Transbaikalia: geological and geophysical structure, types of ore deposits, predictive assessment, and mineral-resource potential, *Geology of Ore Deposits*., 2015, vol. 57, no. 2, pp. 101–110.
https://doi.org/10.1134/S1075701515020026

Gordienko, I.V., Roshchektaev, P.A., Gorokhovsky, D.V., Oka ore district of the Eastern Sayan: geology, structural-metallogenic zonation, genetic types of ore deposits, their geodynamic formation conditions, and outlook for devel-

opment, *Geology of Ore Deposits*., 2016. vol. 58, no. 5, pp. 361–382.
https://doi.org/10.1134/S1075701516050044

Gordienko, I.V. and Tsygankov, A.A., Magmatism and ore formation in different geodynamic settings of the Sayan–Baikal fold area and adjacent territories, *Razvedka Okhr. Nedr,* 2017, no. 9, pp. 36–44.

Ignatovich, V.I., Mineral-raw base of Molybdenum, *Razvedka Okhr. Nedr,* 2007, no. 12, pp. 37–43.

Ignatovich, V.I. and Fil'ko, A.S., *State and prospects of increase of mineral-raw base of molybdenum and tungsten in the Buryat Republic, Khimiya, tekhnologiya i prirodnoe syr'e molibdena i vol'frama* (Chemistrty, Technology, and Natural Raw Material for Molybdenum and Tungsten), Ulan-Ude, 1978, pp. 131–140.

Jahn, B.M., Litvinovsky, B.A., Zanvilevich, A.N., and Reichow, M.K., Peralkaline granitoid magmatism in the Mongolian-Transbaikalian Belt: evolution, petrogenesis and tectonic significance, *Lithos,* 2009, vol. 113, pp. 521–539. http://dx.doi.org/. 2009.06.015
https://doi.org/10.1016/j.lithos

Khrenov, P.M., Komarov, Yu.V., Bukharov, A.A., Gordienko, I.V., et al., *Volcanic belts of southern East Siberia and their ore potential, Voprosy genezisa i zakonomernosti razmeshcheniya endogennykh mestorozhdenii (Genetic Problems and Tendencies in the Distribution of Endogenous Deposits)*, Moscow: Nauka, 1966, pp. 277–315.

Khubanov, V.B., Dugdanova, E.E., Tsygankov, A.A., and Buyantuev, M.D., Age relations of alkaline and molybdenite-bearing granitoids of the Selenga molybdenum ore district, Western Transbaikalia, *Granity i evolyutsiya Zemli: Mater. III Mezhdunar. geol. konf.* (Granites and Evolution of the Earth. Proc. 3rd International Geological Conference), Yekaterinburg, 2017, pp. 330.

Kovalenko, V.I. and Yarmolyuk, V.V., *Evolution of magmatism in the Mongolian structures, Evolyutsiya geologicheskikh protsessov i metallogeniya Mongolii* (Evolution of Geological Processes and Metallogeny of Mongolia), Moscow: Nauka, 1990, pp. 23–54.

Kovalenko V.I., Yarmolyuk V.V., Sal'nikova E.B., et al., Sources of igneous rocks and genesis of the Early Mesozoic tectonomagmatic area of the Mongolia Transbaikalia magmatic region: 2. Petrology and geochemistry, *Petrology,* 2003, vol. 11, no. 3, pp. 205–229.

Kupriyanova, I.I. and Shpanov, E.P., *Berillievye mestorozhdeniya Rossii* (Berillium Deposits of Russia), Moscow: GEOS, 2011.

Kupriyanova, I.I., Shpanov, E.P., and Gal'chenko, V.I., *Ermakovskoe flyuorit-berillievoe mestorozhdenie (Zapadnoe Zabaikal'e, Rossiya)* (Ermakovka Fluorite–Beryllium Deposit (Western Transbaikalia, Russia), Moscow: VIMS. 2009.

Kuzmin, M.I. and Yarmolyuk, V.V., Mantle plumes in northeastern Asia and their role in the formation of endogenous deposits, *Russ. Geol. Geophys.,* 2014, vol. 55, no. 2, pp. 120–143.

Litvinovsky, B.A., Yarmolyuk, V.V., Vorontsov, A.A., Zhuravlev, D.Z., Posokhov, V.F., Sandimirova, G.P., and Kuzmin, D.V., Late Triassic stage of formation of the Mongol-Transbaikalian alkaline-granitoid province: data of isotope-geochemical studies, *Russ. Geol. Geophys.,* 2001, vol. 42, no. 3, pp. 445–456.

Lykhin, D.A., Kovalenko, V.I., Yarmolyuk, V.V., Kotov, A.B., Kovach, V.P., and Sal'nikova, E.B., Age, composition, and sources of ore-bearing magmatism of the Orot beryllium deposit in western Transbaikalia, Russia, *Geol. Ore Deposits,* 2004, vol. 46, no. 2, pp. 108–124.

Lykhin, D.A. and Yarmolyuk, V.V., Magmatism and formation conditions of the Urma helvite–bertrandite deposit, West Transbaikal berillium province, *Geol. Ore Deposits,* 2014, vol. 56, no. 4, pp. 281–301.

Lykhin, D.A. and Yarmolyuk, V.V., *Zapadno-Zabaikal'skaya berillievaya provintsiya: mestorozhdeniya, rudonosnyi magmatizm, istochniki veshchestva* (Western Transbaikalian Beryllium Province: Deposits, Ore-Bearing Magmatism, and Sources), Moscow: GEOS, 2015.

*Mineral'no-syr'evoi potentsial nedr Rossiiskoi Federatsii, vol. 1. Prognozno-metallogenicheskii analiz* (Mineral-Raw Potential of Interiors of the Russian Federation. Volume 1. Forecasting–Metallogenic Analysis), Petrov, O.V, Eds., St. Petersburg: VSEGEI, 2009.

Minina, O.R., Doronina, N.A., Nekrasov, G.E., Vetluzhskikh, L.I., Lantseva,V.S., Aristov, V.A., Naugol'nykh, S.V., Kurilenko, A.V., Khodyreva, E.V., Early Hercynides of the Baikal-Vitim Fold System, Western Transbaikal Region, *Geotectonics*, 2016, vol. 50, no. 3, pp. 276–294.
https://doi.org/10.1134/S0016852116030079

Nikiforov A.V., Yarmolyuk V.V., Kovalenko V.I., Ivanov V.G., Andreeva I.A., and Zhuravlev D.Z., Pozdnemezozoiskie karbonatity Zapadnogo Zabaikal'ya: izotopno-geokhimicheskie kharakteristiki i istochniki, *Petrology,* 2002, vol. 10, no. 2, pp.168–188.

Nikiforov, A.V., Yarmolyuk, V.V., Pokrovskii, B.G., Kovalenko, V.I., Ivanov, V.G., Andreeva, I.A., Zhuravlev, D.Z., Ripp, G.S., Vladykin, N.V., and Korshunov, V.V., Late Mesozoic Carbonatites of Western Transbaikalia:mineralogical, chemical, and isotopic (O, C, S, and Sr) characteristics and relationships to alkaline magmatism, *Petrology,* 2000, vol. 8, no. 3, pp. 278–302.

Novikova, M.I. and Zabolotnaya, N.P., Beryllium feldspatic metasomatites of Mesozoic activation zones, *Sov. Geologiya,* 1988, no. 12, pp. 92–100.

Pekhterev, S.N., Nechepaev, E.V., Artamonova, N.A., Vologdin, M.A., Dukhovskii, A.A., Enikeev, F.I., Kozhunova, S.V., Krutkina, O.N., Stupina, T.A., Chetverikov, M.E., and Shor, G.M., *Gosudarstvennaya geologicheskaya karta Rossiiskoi Federatsii. Masshtab 1 : 1000000 (tret'e pokolenie). Seriya Aldano-Zabaikal'skaya. List M-49. Ob'ytasnitel'naya zapiska* (State Geological map of the Russian Federation. Map 1 : 1000 000 (3rd Generation). Series Aldan–Transbaikalian. Sheet M-49, Explanatory Note), St. Petersburg: VSEGEI, 2012.

Petrov, V.A., Andreeva, O.V., Poluektov, V.V., and Kovalenko, D.V., Tectono-magmatic cycles and geodynamic settings of ore-bearing system formation in the Southern Cis-Argun region, *Geol. Ore Deposits,* 2017, vol. 59, no. 6, pp. 431–452.

Platov, V.S., Savchenko, A.A., Ignatov, A.M., Gorokhovskii, D.V., Shor, G.M., Alekseenko, V.D., Mukhin, V.N., Suslova, S.V., Platova, E.V., Bol'shakova, T.V., and Shelomentseva, T.I., *Gosudarstvennaya geologicheskaya karta Rossiiskoi federatsii. Masshtab 1 : 1000000 (tret'e pokolenie). Aldano-Zabaikal'skaya seriya. List M-48. Ob'ytasnitel'naya zapiska* (State Geological Map of the Russian Federation. Scale 1 : 1000000 (3rd Generation). Aldan–Series. Sheet M-48, Explanatory Note), St. Petersburg: VSEGEI. 2009

Pokalov, V.T., Bolokhontseva, S.V., and Vasin, V.V., Upper Paleozoic Zharchikhinskoe molybdenum occurrence in the breccia pipe in the Caledonides of Western Transbaikalia, *Izv. AN SSSR, Ser. Geol.,* 1985, no. 7, pp. 99–107.

Reichow, M.K., Litvinovsky, B.A., Parrish, R.R., and Saunders, A.D., Multi-stage emplacement of alkaline and peralkaline syenite-granite suites in the Mongolian-Transbaikalian Belt, Russia: Evidence from U-Pb geochronology and whole rock geochemistry, *Chem. Geol.,* 2010, vol. 273, nos. 1–2, pp. 120–135.
https://doi.org/10.1016/j.chemgeo.2010.02.017

Reif, F.G., Phenakite–bretrandite deposits of beryllium, alkaline granites, and their ore productivity, *Problemy geologii, mineral'nykh resursov i geoekologii Zapadnogo Zabaikal'ya: Mater. mezhdunar. nauchno-praktich. konf., posvyashch. 50-letiyu Buryatsk. geol. upravl.* (Problems of Geology, Mineral Resources, and Geoecology of Western Transbaikalia: Proc. International Scientific-Practical Conference Devoted to the 50th Anniversary of the Buryatsk. Geol. Upravl.), Ulan-Ude: 2007, pp. 63–65.

Ripp, G.S., Ermakovka fluorite–phenakite–bertrandite deposit, *Mestorozhdeniya Zabaikal'ya* (Deposits of Transbaikalia), Moscow: Geoinformmark, 1995, vol. 1, book 2, pp. 125–129.

Ripp, G.S., Doroshkevich, A.G., and Posokhov, V.F., Age of carbonatite magmatism in Transbaikalia, *Petrology,* 2009, vol. 17, no. 1, pp.73–89.

Ripp, G.S., Izbrodin, I.A., Lastochkin, E.I., Doroshkevich, A.G., Rampilov, M.O., and Burtseva, M.V., *Oshurkovskii bazitovyi pluton: khronologiya, izotopno-geokhimicheskie i mineralogicheskie osobennosti, usloviya obrazovaniya* (Oshurkovskii Basite Pluton: Chronology, Isotope-Geochemical, and Mineralogical Features, and Conditions of Formation), Novosibirsk: Akademicheskoe izd-vo "Geo", 2013.

Ripp, G.S., Kobylkina, O.V., Doroshkevich, A.G., and Sharakshinov, A.O. *Pozdnemezozoiskie karbonatity Zapadnogo Zabaikal'ya* (Late Mesozoic Carbonatites of Western Transbaikalia), Ulan-Ude: BNTs SO RAN, 2000.

Shcheglov, A.D., *Endogennaya metallogeniya Zabaikal'ya* (Endogenous Metallogeny of Transbaikalia), Leningrad: Nedra, 1966.

Skripkina, V.V., Vernik, V.L., Reif, L.I., Ignatovich, V.I., and Andreev, G.V., New volcanic structure with molybdenum mineralization in Western Transbaikalia, *Dokl. Akad. Nauk SSSR,* 1982, vol. 264, no. 6, pp. 1461–1464.

Takhanova S.S., *Upravlenie nedrami Respubliki Buryatiya* (Management of Interiors of the Buryat Republic), 2017, no. 9, pp. 3–10.

Tsarev, D.I., and Batueva, A.A., *Differentsiatsiya komponentov bazitov pri granitizatsii (na primere Oshurkovskogo apatitovogo mestorozhdeniya, Zapadnoe Zabaikal'e)* (Differentiation of Basite Components during Granitization by the Example of the Oshurkovskoe Apatite Deposits, Western Transbaikalia), Novosibirsk: Geo, 2013.

Tsarev D.I., Khrustalev V.K., Gal'chenko V.I., and Ayurzhanaeva D.Ts. Geology and Genesis of the Cheremshanka Silica Deposit, Western Transbaikal Region, Russia, *Geol. Ore Deposits,* 2007, vol. 49, no. 4, pp. 297–307.

Tsygankov A.A., Burmakina G.N., Khubanov V.B., Buyantuev M.D., Geodynamics of Late Paleozoic batholith-forming processes in Western Transbaikalia, *Petrology*, 2017, vol. 25, no. 4, pp. 396–418.
https://doi.org/10.1134/S0869591117030043

Tsygankov, A.A., Litvinovsky, B.A., Jahn, B.M., Reikov, M., Liu, D.I., Larionov, A.N., Presnyakov, S.L., Lepekhina, E.N., and Sergeev, S.A., sequence of magmatic events in the Late Paleozoic of Transbaikalia, Russia (U-Pb isotope data), *Russ. Geol. Geophys.,* 2010, vol. 51, no. 9, pp. 972–994.

Vernik, V.L. and Ripp G.S., Zharchikhinskoe molibdenovoe mestorozhdenie, *Mestorozhdeniya Zabaikal'ya* (Transbaikalian Deposits), Moscow: Geoinformmark, 1995, vol. 1, book 2, pp. 176–179.

Vorontsov, A.A. and Yarmolyuk, V.V., The evolution of volcanism in the Tugnui–Khilok sector of the Western Transbaikalia rift area in the Late Mesozoic and Cenozoic, *J. Volcanol. Seismol.,* 2007, no. 4, pp. 213–236.

Yalovik, G.A., State and prospects of the development of the mineral-raw base of the Buryat republic up to 2020, *Globus (Geologiya i Biznes),* 2010, no. 5, pp. 14–29.

Yarmolyuk, V.V., Ivanov, V.G., and Kovalenko, V.I., Sources of intraplate magmatism of Western Transbaikalia in the Late Mesozoic–Cenozoic: trace-element and isotope data, *Petrology,* 1998, vol. 6, no. 2, pp. 101–123.

Yarmolyuk, V.V., Kovalenko, V.I., Sal'nikova, E.B., Budnikov, S.V., and Kovach, V.P., Tectono-magmatic zoning, magma sources, and geodynamics of the Early Mesozoic Mongolia–Transbaikal Province, *Geotectonics,* 2002, no. 4, pp. 293–311.

Yarmolyuk V.V., Kozlovsky A.M., Salnikova E.B., Travin A.V., Kudryashova E.A., Riftogenic magmatism of western part of the Early Mesozoic Mongolian-Transbaikalian igneous province: Results of geochronological studies, *Doklady Earth Sciences*, 2017, vol. 475, no. 2, pp. 872–876. https://doi.org/10.1134/S1028334X17080293

Yarmolyuk, V.V., Litvinovsky, B. A., Kovalenko, V.I., Borming Jahn, Zanvilevich, A.N., Vorontsov, V.V., Zhuravlev, D.Z., Posokhov, V.F., Kuz'min, D.V., and Sandimirova, G.P., Formation stages and sources of the peralkaline granitoid magmatism of the northern Mongolia–Transbaikalia rift belt during the Permian and Triassic, *Petrology,* 2001, vol. 9, no. 4, pp. 302–328.

Yarmolyuk, V.V., Vorontsov, A.A., Ivanov, V.G., Kovalenko, V.I., Baikin, D.N., and Sandimirova, G.P., Stages of bimodal and alkaline granite magmatism in the western Transbaikal region: geochronological data on rocks from the Tugnui Depression, *Dokl. Earth Sci.,* 2000, vol. 373, no. 1, pp. 811–815.

Zaitsev, S.U., Main features of localization of uranium mineralization in shale complexes of the Naran area, *Uran: geologiya, resursy, proizvodstvo: tezisy Tret'ego mezhdunarodnogo simpoziuma* (Uranium: Geology, Resources, and Production. Proc. 3rd International Symposium), Moscow: VIMS, 2013, pp. 54.

Zonenshain, L.R., Kuzmin, M.I., and Natapov, L.M., *Tektonika litosfernykh plit territorii SSSR* (Tectonics of Lithospheric Plates of the USSR Territory), Mosciw: Nedra, 1990, vol. 2.

*Translated by E. Murashova*